International Journal of Computational Methods
Vol. 5, No. 2 (2008) 199–236
© World Scientific Publishing Company

World Scientific
www.worldscientific.com

# A GENERALIZED GRADIENT SMOOTHING TECHNIQUE AND THE SMOOTHED BILINEAR FORM FOR GALERKIN FORMULATION OF A WIDE CLASS OF COMPUTATIONAL METHODS

G. R. LIU

*Centre for Advanced Computations in Engineering Science*
*Department of Mechanical Engineering*
*National University of Singapore*
*9 Engineering Drive 1, Singapore 117576*

*Singapore-MIT Alliance (SMA), E4-04-10*
*4 Engineering Drive 3, Singapore 117576*

Received 7 November 2007
Accepted 29 April 2008

This paper presents a generalized gradient smoothing technique, the corresponding smoothed bilinear forms, and the smoothed Galerkin weakform that is applicable to create a wide class of efficient numerical methods with special properties including the upper bound properties. A generalized gradient smoothing technique is first presented for computing the smoothed strain fields of displacement functions with discontinuous line segments, by "rudely" enforcing the Green's theorem over the smoothing domain containing these discontinuous segments. A smoothed bilinear form is then introduced for Galerkin formulation using the generalized gradient smoothing technique and smoothing domains constructed in various ways. The numerical methods developed based on this smoothed bilinear form will be spatially stable and convergent and possess three major important properties: (1) it is variationally consistent, if the solution is sought in a Hilbert space; (2) the stiffness of the discretized model will be reduced compared to the model of the finite element method (FEM) and often the exact model, which allows us to obtain upper bound solutions with respect to both the FEM solution and the exact solution; (3) the solution of the numerical method developed using the smoothed bilinear form is less insensitive to the quality of the mesh, and triangular meshes can be used perfectly without any problems. These properties have been proved, examined, and confirmed by the numerical examples. The smoothed bilinear form establishes a unified theoretical foundation for a class of smoothed Galerkin methods to analyze solid mechanics problems for solutions of special and unique properties: the node-based smoothed point interpolation method (NS-PIM), smoothed finite element method (SFEM), node-based smoothed finite element method (N-SFEM), edge-based smoothed finite element method (E-SFEM), cell-based smoothed point interpolation method (CS-PIM), etc.

*Keywords*: Elasticity; point interpolation method; finite element method; meshfree method; solution bound; smoothing operation; bilinear form; variational principle; Galerkin weakform; numerical method.

## 1. Introduction

To solve engineering problems, many powerful numerical methods have been developed, such as the Finite Element Method (FEM) [Hughes (1987); Liu and Quek (2003)], Finite Difference Method (FDM), and recently Meshfree Methods (see, e.g. [Liu and Liu (2003); Liu (2002)]). The FEM is well developed, has a solid foundation on the variational principles, and is currently the most widely used reliable numerical approach with many commercial software packages available. However, there are three major issues need to be resolved in order to better meet the demands in solving practical engineering problems in more efficient and convenient manner.

The first issue is the "over-stiff" phenomenon of a fully-compatible FEM model of assumed displacement, which can have consequences of (1) the so-called "locking" behavior for many problems, and (2) inaccuracy in stress solutions. The second issue concerns with the mesh distortion related problems such as the significant accuracy loss when the element mesh is heavily distorted. The third issue is the mesh generation. We, engineers, often prefer using triangular types of mesh as they can be created much more easily and even automatically. However, it is well-known that the FEM does not like such elements and often give solutions of very poor accuracy.

The over-stiff phenomenon is attributed to nature of the fully compatible displacement approach. Many efforts have been made in resolving this issue, especially in the area of hybrid FEM formulations (see, e.g. [Pian and Wu (2006)]). Improvements on FEM also carried out for fluid flow problems [Ortega *et al.* (2007)]. Recently, a so-called $\alpha$-FEM [Liu, Nguyen and Lam (2008b)] has been developed by scaling the gradient of strains with a scaling factor so as to provide a proper "softness" to the model. The $\alpha$-FEM can not only give much more accurate solution in stresses, but also produce "nearly" exact solution in energy norm for a class of problems, with very little change to the standard FEM formulation and codes. It also offers simple and practical ways to resolve some locking problems. Liu *et al.* has also discovered an important fact that the $\alpha$-FEM is NOT *variationally consistent*, and yet it can *always* (not by any chance) produce much better solution than the FEM that is perfectly variationally consistent! This finding opens an important window for the development of a new class of methods via manipulating the strain field obtained directly from the assumed displacements using the compatibility equation. We now CAN commit *variational crime*, as long as we have proper ways to control the assumed strain field so that the solution can be *somehow* bounded, so that the solution will be convergent (even monotonically) when certain consistence of the assumed primary (displacement) variable is provided.

A smoothed FEM (or SFEM) [Liu, Dai and Nguyen (2007)] has also been formulated recently by combining the FEM procedures and the *gradient smoothing operation* that is known as distributional derivatives in classic sense. The smoothing operation has been used in the nonlocal continuum mechanics [Eringen and

Edelen (1972)], the smoothed particle hydrodynamics (SPH) [Lucy (1977); Monaghan (1982); Liu and Liu (2003)], in resolving the material instabilities [Chen and Belytschko (2000)] and spatial instability in nodal integrated meshfree methods and restoring conformability [Chen *et al.* (2001)], and obtaining upper bound solution and restoring conformability in meshfree point interpolation methods [Liu *et al.* (2005); Zhang *et al.* (2007)]. The SFEM works very effective for solid mechanics problems including dynamic problems, can also produce much more accurate stress solution, and n-sided polygonal elements and very heavily distorted mesh can be used [Liu *et al.* (2007b)]. Detailed theoretical aspects including stability and convergence about SFEM can be found in [Dai *et al.* (2007)]. The study of SFEM has also clearly shown that the smoothing operation on strains controls the assumed strain field in a proper fashion to ensure the stability (boundness) and hence the (monotonic) convergence, and ultimately gives the SFEM some very good features. This is done again with a very little change to the standard FEM formulation and codes.

In the other front of development related to meshfree methods, the node-based smoothed point interpolation method (NS-PIM)[a] has been developed recently [Liu *et al.* (2005); Zhang *et al.* (2007)] using the node-based smoothing operations [Chen *et al.* (2001)]. The NS-PIM is formulated using PIM [Liu (2002); Liu and Gu (2001)] or RPIM [Wang and Liu (2002)] shape functions possible of discontinuous and with the Delta function property for easy treatment of essential boundary conditions. It was found that NS-PIM or (NS-RPIM [Liu *et al.* (2006)]) is at least linearly conforming (always pass the standard patch tests when linear displacements on the boundary are enforced), can produce much better stress solution, much more tolerant to mesh distortion, works very well for triangular elements, and more importantly it provides upper bound solution in energy norm. Based on the idea of NS-PIM and SFEM, a node-based SFEM (or N-SFEM) has also been formulated. The N-SFEM can be viewed as a special case of NS-PIM, but based on n-sided polygonal element mesh [Liu *et al.* (2007a,b)], and has quite similar properties as NS-PIM. These works have sent a very clear message that node-based smoothing operation can offer upper bound solutions for general solid mechanics problems. It is found that NS-PIM and N-SFEM can produce the so-called spurious modes when they are used for solving dynamic problems. This is due to their "overly-softness" introduced by the excessive node-based smoothing operation, leading to temporal instability. To overcome this problem, a very effective edge-based smoothed FEM (E-SFEM) has been recently formulated [Liu, Nguyen and Lam (2008a)]. The E-SFEM not only produces accurate solution, but also is temporally stable and no spurious modes and hence works very well for dynamic problems.

[a]The NS-PIM was originally termed as the linearly conforming point interpolation method (LC-PIM), because it is at least linearly conforming. We changed the name because the later formulations of cell-based and edge-based smoothing techniques those are all at least linearly conforming, but distinct in the creation of smoothing domains.

In this work, we introduce a generalized gradient smoothing technique, the corresponding smoothed bilinear form and the Galerkin formulation for computational methods using both continuous and discontinuous assumed displacement functions. We then prove the important general properties of the bilinear form, and use it to formulate a Galerkin weakform that is applicable to establish a class of effective numerical methods. The smoothed bilinear form offers a unified theoretical foundation for this class of methods that possess some desired superior properties such as the upper bound property (in energy norm) for solid mechanics problems.

The numerical methods developed based on this smoothed bilinear form will possess three major important properties: (1) it is variationally consistent, if the solution is sought in a Hilbert space; (2) the stiffness of the discretized model will be reduced compared to the FEM model and often the exact model, which allows us to obtain upper bound solutions with respect to both the FEM solution and the exact solution; (3) the solution of a numerical method developed using the smoothed bilinear form are insensitive to the quality of the mesh, and triangular meshes can be used perfectly without any problems. These properties have been proven and confirmed by numerical results of SFEM [Dai *et al.* (2007)], N-SFEM [Liu *et al.* (2007a,b)], NS-PIM [Liu and Zhang (2005, 2008)], and the E-SFEM [Liu, Nguyen and Lam (2008a)].

Our formulation will be largely for two-dimensional (2D) problems. Its extension to 3D and reduction to 1D is straightforward with changes only in dimension and rotations.

## 2. Brief on Basic Equations

We first brief the basic equations for solid mechanics problem of linear elasticity, for which different weakforms will be established. Consider a two-dimensional solid mechanics problem with a physical domain of $\Omega \in \Re^2$ bounded by $\Gamma$. In this paper, we speak of open domain $\Omega$, meaning that the boundary $\Gamma$ of the domain is not included, unless otherwise indicated. The static equilibrium equation for 2D solids in the domain $\Omega \in \Re^2$ can be written as

$$\frac{\partial \sigma_{ij}}{\partial x_j} + b_i = 0, \quad i, j = 1, 2, \tag{1}$$

where $b_i$ are given external body force and $\sigma_{ij}$ is the stress tensor which relates to the strains tensor $\varepsilon_{ij}$ via the constitutive equation or the Generalized Hook's law:

$$\sigma_{ij} = C_{ijkl}\varepsilon_{kl}, \tag{2}$$

where $C_{ijkl}$ is elasticity tensor of material property constants that are symmetrical:

$$C_{ijkl} = C_{jikl} = C_{ijlk} = C_{klij}. \tag{3}$$

The strains tensor $\varepsilon_{ij}$ relates to the displacements by the following compatibility equation.

$$\varepsilon_{kl} = \frac{1}{2}\left(\frac{\partial u_k}{\partial x_l} + \frac{\partial u_l}{\partial x_k}\right), \tag{4}$$

where $u_i$, $i = 1, 2$ is the displacement components in the $x_i$-directions at a point in $\Omega$.

In matrix form, the equilibrium Eq. (1) becomes (see, e.g. [Liu and Quek (2003)])

$$\mathbf{L}_d^T \boldsymbol{\sigma} + \mathbf{b} = \mathbf{0}. \tag{5}$$

where

$$\mathbf{L}_d \left( \frac{\partial}{\partial x_1}, \frac{\partial}{\partial x_2} \right) = \begin{bmatrix} \dfrac{\partial}{\partial x_1} & 0 \\ 0 & \dfrac{\partial}{\partial x_2} \\ \dfrac{\partial}{\partial x_2} & \dfrac{\partial}{\partial x_1} \end{bmatrix}. \tag{6}$$

The constitutive equation becomes

$$\boldsymbol{\sigma} = \mathbf{C}\boldsymbol{\varepsilon}, \tag{7}$$

where $\mathbf{C}$ is matrix of material properties which entries of $C_{ijkl}$, $\boldsymbol{\sigma} = \{\sigma_{11}, \sigma_{22}, \sigma_{12}\}^T$ and $\boldsymbol{\varepsilon} = \{\varepsilon_{11}, \varepsilon_{22}, \varepsilon_{12}\}^T$. The compatibility equation (4) can also be written in the matrix form of

$$\boldsymbol{\varepsilon} = \mathbf{L}_d \mathbf{u}, \tag{8}$$

where $\mathbf{u} = \{u_1, u_2\}^T$ is the displacement vector. Substituting Eq. (8) into (7) and then into (5), we have

$$\mathbf{L}_d^T \mathbf{C} \mathbf{L}_d \mathbf{u} + \mathbf{b} = \mathbf{0}. \tag{9}$$

The boundary conditions can be two types: Dirichlet boundary condition and Neumann boundary condition. Let $\Gamma_D$ denote a part of $\Gamma$, on which homogenous Dirichlet boundary condition is specified, we then have

$$u_i = 0, \quad \text{on } \Gamma_D \in \Gamma. \tag{10}$$

Let $\Gamma_N$ denotes a part of $\Gamma$, on which Neumann boundary condition is satisfied,

$$\sigma_{ij} n_j = t_i, \quad \text{on } \Gamma_N \in \Gamma, \tag{11}$$

where $n_j$ is unit outward normal vector, and $t$ is the specified boundary stress on $\Gamma_N$, respectively. The matrix form of Eq. (11) is as follows:

$$\mathbf{L}_n^T \sigma = \mathbf{t}, \quad \text{on } \Gamma_N \in \Gamma, \tag{12}$$

where

$$\mathbf{L}_n(n_x, n_y) = \begin{bmatrix} n_x & 0 \\ 0 & n_y \\ n_y & n_x \end{bmatrix}. \tag{13}$$

The matrix form of equations is helpful and will also be used in the following sections.

## 3. Brief on Weak Form Formulation

We shall now brief the standard weak form formulation for linear elasticity problem of 2D solids. More details can be found in [Hughes (1987)]. To begin, we introduce a functional space

$$\mathbb{S} = \{v \in H^1(\Omega) | v_i = 0 \text{ on } \Gamma_D\}, \tag{14}$$

where $H^1(\Omega)$ is a Hilbert space. By multiplying Eq. (1) with a test function $v \in \mathbb{S}$ and performing integration over the entire domain $\Omega$, we have

$$\int_\Omega v_i \frac{\partial \sigma_{ij}}{\partial x_j} d\Omega + \int_\Omega b_i v_i d\Omega = 0, \quad v \in \mathbb{S} \tag{15}$$

where $i, j = 1, 2$. Applying green divergence theorem yields

$$\int_\Omega \frac{\partial v_i}{\partial x_j} \sigma_{ij} d\Omega - \int_{\Gamma_N} v_i \sigma_{ij} n_j d\Gamma - \int_\Omega b_i v_i d\Omega = 0. \tag{16}$$

Substituting Eqs. (2) and (4) into the above equation leads to

$$\underbrace{\int_\Omega \frac{\partial v_i}{\partial x_j} \left( C_{ijkl} \frac{\partial u_k}{\partial x_l} \right) d\Omega}_{a(u,v)} = \underbrace{\int_{\Gamma_N} v_i \sigma_{ij} n_j d\Gamma + \int_\Omega b_i v_i d\Omega}_{f(v)}. \tag{17}$$

We now have the well-known bilinear form:

$$a(w, v) = \int_\Omega \frac{\partial v_i}{\partial x_j} \left( C_{ijkl} \frac{\partial w_k}{\partial x_l} \right) d\Omega, \tag{18}$$

that has basic properties of symmetry and positivity. The linear functional

$$f(v) = \int_{\Gamma_N} v_i t_i d\Gamma + \int_\Omega b_i v_i d\Omega. \tag{19}$$

It follows from Eq. (17) that the exact solution of the displacement $u \in \mathbb{S}$ satisfies

$$a(u, v) = f(v), \quad \forall\, v \in \mathbb{S}, \tag{20}$$

where $u$ is the "exact" displacement field of a given problem that satisfies strong form Eqs. (1), (10) and (11).

## 4. Brief on the Finite Element Method (FEM)

In practice, it is generally very difficult to solve the governing equations either in strong or weak forms in analytical means for the *exact* solution. We then often resort to numerical methods to obtain *approximate* solutions. The most popular method is the traditional finite element method (FEM) based on the weak form formulation where the Galerkin projection is chosen to obtain an approximate solution $\tilde{u}$. It is well known that such a FEM solution is the best (in energy norm) possible solution in the discrete finite element space $\tilde{\mathbb{S}}$ (see, e.g. [Hughes (1987)]), that $\tilde{u} \to u$ when $\tilde{\mathbb{S}} \to \mathbb{S}$, meaning that the approximate FEM solution will approach to the exact

solution when the size of element approaches to zero and the dimension of the FEM model $\aleph \to \infty$.

The finite element solution $\tilde{u}$ satisfies

$$a(\tilde{u}, \upsilon) = f(\upsilon), \quad \upsilon \in \tilde{\mathbb{S}}, \tag{21}$$

where displacement field $\tilde{u} \in \tilde{\mathbb{S}}$ is expressed in terms of the following interpretation,

$$\tilde{u}(\mathbf{x}) = \sum_{i=1}^{\aleph} \tilde{d}_i \varphi_i(\mathbf{x}), \tag{22}$$

where $\mathbf{x} = \{x_1, x_2\}^T$, $\tilde{d}_i$ is a nodal displacement, and $\varphi_i \in \tilde{\mathbb{S}}$ is a nodal basis function (or element shape functions) which has the Delta function property: $\varphi_i(\mathbf{x}_j) = \delta_{ij}$ at node $i$, and evaluated at coordinate $\mathbf{x}_j$.

We then substitute Eq. (22) into Eq. (21), and set $\varphi_i$, $i = 1, \ldots, \aleph$, as the test function $\upsilon$, we have the following discrete set of $\aleph$ equations.

$$\sum_{j=1}^{\aleph} a(\varphi_j, \varphi_i)\tilde{d}_j = f(\varphi_i), \quad i = 1, \ldots, \aleph, \tag{23}$$

which can be written in the matrix form of

$$\tilde{\mathbf{K}}\tilde{\mathbf{d}} = \tilde{\mathbf{f}}, \tag{24}$$

where $\tilde{\mathbf{K}}$ is the FEM stiffness matrix with entries of $\tilde{K}_{ij} = a(\varphi_j, \varphi_i)$, $1 \le i, j \le \aleph$, $\tilde{\mathbf{d}}$ is the vector of nodal displacements $\tilde{d}_i$, and $\tilde{\mathbf{f}}$ is the vector with entries of $\tilde{f}_i = f(\varphi_i)$.

We now state some of the well-known, useful and important properties of FEM.

**Remark 4.1.** *Lower Bound Property*: The strain energy related to fully compatible FEM solution is a lower bound of the exact strain energy.

$$U(\tilde{\varepsilon}) = \frac{1}{2}a(\tilde{u}, \tilde{u}) \le \frac{1}{2}a(u, u) = U(\varepsilon) \tag{25}$$

where $\tilde{\varepsilon} = \mathbf{L}_d\tilde{\mathbf{u}}$ is the strains obtained using the FEM displacements $\tilde{u} \in \tilde{\mathbb{S}} \subset \mathbb{S}$, $\varepsilon = \mathbf{L}_d\mathbf{u}$ is the exact strain obtained using the exact displacements $u \in \mathbb{S}$, and $U(\varepsilon)$ is the strain energy of the system defined as

$$U(\varepsilon) = \frac{1}{2}\int_\Omega \varepsilon^T \mathbf{C}\varepsilon \, d\Omega. \tag{26}$$

For the FEM model, the strain energy can be evaluated using any of the following expressions.

$$U(\tilde{\varepsilon}) = \frac{1}{2}\int_\Omega \tilde{\varepsilon}^T \mathbf{C}\tilde{\varepsilon} \, d\Omega = \frac{1}{2}a(\tilde{u}, \tilde{u}) = \frac{1}{2}\tilde{\mathbf{d}}^T\tilde{\mathbf{K}}\tilde{\mathbf{d}} \tag{27}$$

and for the exact model we should have

$$U(\varepsilon) = \frac{1}{2}\int_\Omega \varepsilon^T \mathbf{C}\varepsilon \, d\Omega = \frac{1}{2}a(u, u). \tag{28}$$

The proof of the lower bound property can be found in a number of references, for example [Hughes (1987)] in variational formulation and [Liu and Zhang (2008)] in

matrix formulation based on energy principle. The lower bound property implies the well-known fact that the FEM solution underestimates the strain energy. This is equivalent to say that the FEM solution overestimates the total potential energy. This property of FEM provides a good global measure of the lower bound of the FEM solution.

**Remark 4.2.** *Monotonic convergence property*: For given a sequence of $n_m$ *nested* element meshes $M_1, M_2, \ldots, M_{n_m}$, such that the corresponding solution spaces satisfies $\tilde{\mathbb{S}}_{M_1} \subset \tilde{\mathbb{S}}_{M_2} \cdots \subset \tilde{\mathbb{S}}_{M_{n_m}} \subset \hat{\mathbb{S}}$, then the following inequalities stand

$$U(\tilde{\boldsymbol{\varepsilon}}_{M_1}) \leq U(\tilde{\boldsymbol{\varepsilon}}_{M_2}) \leq \cdots \leq U(\tilde{\varepsilon}_{M_{n_m}}) \leq U(\varepsilon), \tag{29}$$

where $\tilde{\boldsymbol{\varepsilon}}_{m_i}$ is the FEM compatible solution of strains obtained using mesh $m_i$. This property can be shown easily using the arguments give by Oliveira [1968].

**Remark 4.3.** *Reproducibility of FEM*: If $\mathbf{u} \in \tilde{\mathbb{S}}$, the then the FEM will reproduce the exact solution $u$. This property can easily be proven [Liu and Quek (2003); Oliveira (1968)].

## 5. A Smoothed Bilinear Form

### 5.1. *Function and gradient approximation*

We first introduce integral representation of a function (see, e.g. [Liu (2002)]):

$$w^{IR}(\mathbf{x}) = \int_{\Omega_{\mathbf{x}}} w(\boldsymbol{\xi})\, \widehat{W}\,(\mathbf{x} - \boldsymbol{\xi}) \mathrm{d}\boldsymbol{\xi} \tag{30}$$

where the superscript "*IR*" stands for integral representation, and $\widehat{W}$ is a predescribed smoothing function defined in the smoothing domain $\Omega_{\mathbf{x}} \subset \Omega$ for the point at $\mathbf{x}$, as shown in Fig. 1. Note that the smoothing domain is "moving" and hence domains for different $\mathbf{x}$ can overlap. The smoothing function can also be different for different $\mathbf{x}$. For a $w \in \mathbb{S}$ the integral representation can also be done for the first derivatives of a function.

$$\left(\frac{\partial w_i(\mathbf{x})}{\partial x_j}\right)^{IR} = \int_{\Omega_{\mathbf{x}}} \frac{\partial w_i(\boldsymbol{\xi})}{\partial x_j}\, \widehat{W}\,(\mathbf{x} - \boldsymbol{\xi}) \mathrm{d}\boldsymbol{\xi}. \tag{31}$$

Note that Eqs. (30) and (31) are standard forms of *smoothing operations*. These forms was used in the nonlocal continuum mechanics [Eringen and Edelen (1972)], the smoothed particle hydrodynamics [Lucy (1977); Monaghan (1982)], stabilizing nodal integrated meshfree methods and restoring conformability [Chen *et al.* (2001)], and restoring conformability and obtaining upper bound solution in meshfree point interpolation methods [Liu and Zhang (2008)]. Using Green's divergence theorem, Eq. (31) becomes

$$\left(\frac{\partial w_i(\mathbf{x})}{\partial x_j}\right)^{IR} = \int_{\Gamma_{\mathbf{x}}} w_i(\boldsymbol{\xi}) n_j\, \widehat{W}(\mathbf{x} - \boldsymbol{\xi}) \mathrm{d}\Gamma - \int_{\Omega_{\mathbf{x}}} w_i(\boldsymbol{\xi}) \frac{\partial\, \widehat{W}(\mathbf{x} - \boldsymbol{\xi})}{\partial x_j} \mathrm{d}\boldsymbol{\xi} \tag{32}$$

where $n_j$ is the directional cosine of the outwards normal on $\Gamma_{\mathbf{x}}$.

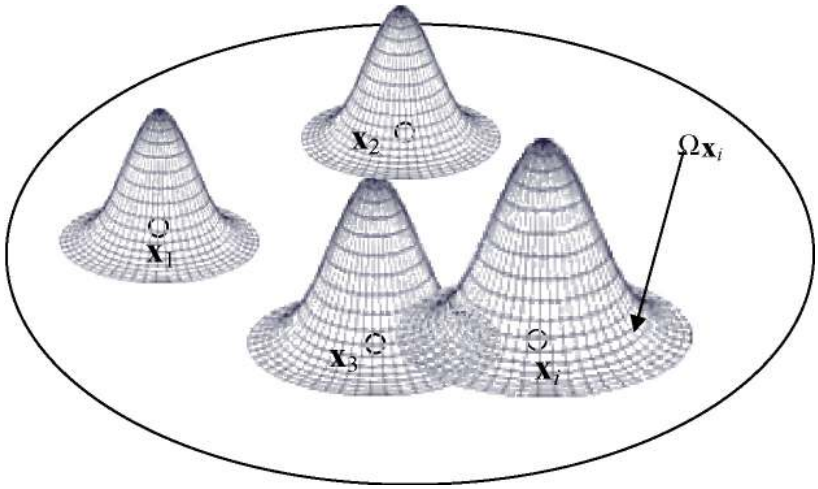


Fig. 1. Moving smoothing domains $\Omega_{\mathbf{x}}$ for integral representation of a function at $\mathbf{x}$, over which the smooth function is defined. Note that the smoothing domain can be different for different $\mathbf{x}$ and they can overlap. The smoothing functions can also be different for different $\mathbf{x}$.

### 5.2. *Generalized gradient smoothing technique*

Note that Eq. (32) requires $w$ being continuous and hence it is at least piecewisely differentiable, as per the original Green's divergence theorem. If $w$ is discontinuous in $\Omega_{\mathbf{x}}$,

$$\int_{\Omega_{\mathbf{x}}} \frac{\partial w_i(\xi)}{\partial x_j} \widehat{W}(\mathbf{x}-\boldsymbol{\xi}) d\boldsymbol{\xi} \neq \int_{\Gamma_{\mathbf{x}}} w_i(\boldsymbol{\xi}) n_j \widehat{W}(\mathbf{x}-\boldsymbol{\xi}) \mathrm{d}\Gamma - \int_{\Omega_{\mathbf{x}}} w_i(\boldsymbol{\xi}) \frac{\partial \widehat{W}(\mathbf{x}-\boldsymbol{\xi})}{\partial x_j} \mathrm{d}\boldsymbol{\xi} \quad (33)$$

We however, "rudely" use Eq. (32) to approximate the gradient of $w$, for discontinuous $w$ in $\Omega_{\mathbf{x}}$:

$$\left(\frac{\partial w_i(\mathbf{x})}{\partial x_j}\right)^{IR} \approx \int_{\Gamma_{\mathbf{x}}} w_i(\boldsymbol{\xi}) n_j \widehat{W}(\mathbf{x}-\boldsymbol{\xi}) \mathrm{d}\Gamma - \int_{\Omega_{\mathbf{x}}} w_i(\boldsymbol{\xi}) \frac{\partial \widehat{W}(\mathbf{x}-\boldsymbol{\xi})}{\partial x_j} \mathrm{d}\boldsymbol{\xi} \quad (34)$$

This generalization is not rigorous in theory, but it is possible in implementation because no differentiation upon $w$ is required on the right-hand-side of Eq. (34). Using Eq. (34) for discontinuous functions can be essentially viewed as "somehow" making the discontinuous function continuous over $\Omega_{\mathbf{x}}$ but keeping the function values on the boundary $\Gamma_{\mathbf{x}}$ unchanged. Therefore, in our later definition of smoothed bilinear forms, we can still "pretend" that the functions are continuous in $\Omega_{\mathbf{x}}$ and hence are in a Hilbert space. This generalization is useful and very important for develop new numerical methods. It allows us to "make" discontinuous functions continuous, approximate the gradients of discontinuous functions conveniently, and

then use them in the Galerkin weak forms as per normal. This generalization makes it possible to use a much wide range of meshfree shape functions such as those PIM and radial PIM shape functions detailed in the books by Liu (2002) and Liu and Gu (2005) for numerical methods based on Galerkin weak forms.

### 5.3. *Generalized bilinear form using moving smoothing domains*

We first define a $G^1$ space. Consider a domain $\Omega$ discretized with $N_e$ subdomains (called cells or elements) $\Omega = \bigcup_{q=1}^{N_e} \Omega_q$ with a set of $N_n$ nodes and $N_l$ line segments $\Gamma_l$ that bound the elements. The $G^1$ spaces are defined as

$$\mathbb{G}^1(\Omega) = \left\{ \begin{array}{l} v \in \mathbb{L}^2(\Omega) \;\Big|\; v(\mathbf{x}) = \sum_{n=1}^{N_n} \phi_n(\mathbf{x}) v_n, \phi_n(\mathbf{x}) (n = 1, ..., N_n) \text{ form a basis,} \\ \qquad\qquad v_n\text{: nodal value of } v \end{array} \right\}$$

Clearly, the $G^1$ spaces allows functions to discontinuous along line segments $\Gamma_l$, and it is a host space of the corresponding $H^1$ space. We further note

$$\mathbb{G}_0^1(\Omega) = \{v \in \mathbb{G}^1(\Omega) | v_i = 0 \text{ on } \Gamma_D\}$$

The *general* continuous bilinear form $\widehat{a}(w, v)$ can be written as

$$\widehat{a}(w,v) = \int_\Omega \left[ \underbrace{\left( \int_{\Omega_\mathbf{x}} \frac{\partial v_i(\boldsymbol{\xi})}{\partial x_j} \widehat{W}(\mathbf{x} - \boldsymbol{\xi}) d\boldsymbol{\xi} \right)}_{\left(\frac{\partial v_i}{\partial x_j}\right)^{IR}} C_{ijkl} \underbrace{\left( \int_{\Omega_\mathbf{x}} \frac{\partial w_k(\boldsymbol{\xi})}{\partial x_l} \widehat{W}(\mathbf{x} - \boldsymbol{\xi}) d\boldsymbol{\xi} \right)}_{\left(\frac{\partial w_k}{\partial x_l}\right)^{IR}} \right] d\Omega, \tag{35}$$

where $v$, $w \in \mathbb{G}^1(\Omega)$. When Eq. (32) is used, we allow $v$ and $w$ being discontinuous at segments in $\Omega$ and treat them as a function in $\mathbb{S}$ as long as these discontinuous segments are covered by smoothing domains, as discussed in Sec. 5.2. Because the gradients of the functions are replaced by the smoothed gradients, we term the bilinear from as *smoothed bilinear form*. Generally, the choice of $\widehat{W}$ will affect the property of $\widehat{a}(w, v)$, and in this paper we require the $\widehat{W}$ satisfy the following basic conditions:

$$\widehat{W}(\mathbf{x} - \boldsymbol{\xi}) \geq 0, \quad \forall \boldsymbol{\xi} \in \Omega_\mathbf{x}, \quad \text{(positivity)} \tag{36}$$

$$\int_{\Omega_\mathbf{x}} \widehat{W}(\mathbf{x} - \boldsymbol{\xi}) d\boldsymbol{\xi} = 1, \quad \text{(unity)} \tag{37}$$

$$\widehat{W}(\mathbf{x} - \boldsymbol{\xi}_1) \leq \widehat{W}(\mathbf{x} - \boldsymbol{\xi}_2), \quad \forall \boldsymbol{\xi}_1, \boldsymbol{\xi}_2 \in \Omega_\mathbf{x} \quad \text{and} \quad |\mathbf{x} - \boldsymbol{\xi}_1| \leq |\mathbf{x} - \boldsymbol{\xi}_2|, \quad \text{(decay)} \tag{38}$$

The unity ensures that at least the function value at $\mathbf{x}$ can be exactly represented (see, e.g. [Liu and Liu (2003)]). With conditions of unity, we should have the following remarks.

**Remark 5.4.** *Reproducing Property*: When $\widehat{W}$ satisfies Eq. (37) in the moving smoothing domain $\Omega_{\mathbf{x}}$, the integral representation will be exact: $(\frac{\partial w_i}{\partial x_j})^{IR} = \frac{\partial w_i}{\partial x_j}$, and hence $\widehat{a}(w, \upsilon) = a(w, \upsilon)$.

For simplicity and convenience of the discussion in this paper, we now confine ourselves using the following special smoothing function that is a local constant.

$$\widehat{W}(\mathbf{x} - \boldsymbol{\xi}) = \bar{W}(\mathbf{x} - \boldsymbol{\xi}) = \begin{cases} 1/A_{\mathbf{x}} & \boldsymbol{\xi} \in \Omega_{\mathbf{x}} \\ 0 & \boldsymbol{\xi} \notin \Omega_{\mathbf{x}} \end{cases} \tag{39}$$

where $A_{\mathbf{x}} = \int_{\Omega_{\mathbf{x}}} d\Omega$ is the area of smoothing domain the point at $\mathbf{x}$. It is clear that $\widehat{W}(\mathbf{x} - \boldsymbol{\xi})$ given above satisfies the conditions of unity, positivity and decay, and $\widehat{a}(w, \upsilon)$ becomes

$$\bar{a}(w, \upsilon) = \int_{\Omega} \left[ \underbrace{\left( \frac{1}{A_{\mathbf{x}}} \int_{\Omega_{\mathbf{x}}} \frac{\partial \upsilon_i(\boldsymbol{\xi})}{\partial x_j} d\boldsymbol{\xi} \right)}_{\overline{\frac{\partial \upsilon_i}{\partial x_j}}} C_{ijkl} \underbrace{\left( \frac{1}{A_{\mathbf{x}}} \int_{\Omega_{\mathbf{x}}} \frac{\partial w_k(\boldsymbol{\xi})}{\partial x_l} d\boldsymbol{\xi} \right)}_{\overline{\frac{\partial w_k}{\partial x_l}}} \right] d\Omega, \tag{40}$$

which is an *averaged* form of our continuous smoothed bilinear form. It can be re-written as

$$\begin{aligned} \bar{a}(w, \upsilon) &= \int_{\Omega} \frac{1}{A_{\mathbf{x}}} \left( \int_{\Omega_{\mathbf{x}}} \frac{\partial \upsilon_i(\boldsymbol{\xi})}{\partial x_j} d\boldsymbol{\xi} \right) C_{ijkl} \left( \frac{1}{A_{\mathbf{x}}} \int_{\Omega_{\mathbf{x}}} \frac{\partial w_k(\boldsymbol{\xi})}{\partial x_l} d\boldsymbol{\xi} \right) d\Omega \\ &= \int_{\Omega} \overline{\frac{\partial \upsilon_i}{\partial x_j}} C_{ijkl} \overline{\frac{\partial w_k}{\partial x_l}} d\Omega, \end{aligned} \tag{41}$$

where

$$\overline{\frac{\partial \upsilon_i}{\partial x_j}} = \frac{1}{A_{\mathbf{x}}} \int_{\Omega_{\mathbf{x}}} \frac{\partial \upsilon_i(\boldsymbol{\xi})}{\partial x_j} d\boldsymbol{\xi} = \frac{1}{A_{\mathbf{x}}} \int_{\Gamma_{\mathbf{x}}} \upsilon_i(\boldsymbol{\xi}) n_j \mathrm{d}\Gamma, \tag{42}$$

are the locally averaged gradient at point $\mathbf{x}$ in $\Omega_{\mathbf{x}}$. Since $\Omega_{\mathbf{x}}$ changes with $\mathbf{x}$, the averaged gradient is still a function of $\mathbf{x}$. Again, we use Eq. (42) even if $\upsilon$ is not continues in $\Omega_{\mathbf{x}}$. We note that the reproducing property holds for $\bar{a}(w, \upsilon)$.

**Remark 5.5.** *Reproducing property*: Because satisfies Eq. (37) in the moving smoothing domain $\Omega_{\mathbf{x}}$, the integral representation will be exact: $\overline{\frac{\partial w_i}{\partial x_j}} = \frac{\partial w_i}{\partial x_j}$, and hence $\bar{a}(w, \upsilon) = a(w, \upsilon)$.

Note that the use of moving domain can easily reproduce the original bilinear form. All one needs is to have $\bar{W}$ with unity property. The moving smoothing bilinear form is useful when one needs to reduce the consistence requirement on filed functions, as shown in Eq. (32): the differentiation is now shifted onto the smoothing function.

Another interesting application of moving smoothing domain is to construct continuous strain fields, where moving smoothing domains are used to obtain strains at points in the problem domain, and the point interpolation method is used to construct continuous strain fields to achieve super-convergence, even using linear triangular mesh. This paper will not discuss in this direction further. Instead, we will discuss in more detail on the models that use of stationary smoothing domains.

### 5.4. *Generalized bilinear form using stationary smoothing domains*

In practical formulation of a numerical method, we often need to determine a way to construct stationary smoothing domains that are fixed for a point of interest. Generally, stationary domains can overlap, as shown in Fig. 2.

For the convenience in this study, we do not allow the smoothing domains overlap, and the smoothing domains are constructed based on an arbitrary manner as long as $\Omega = \bigcup_{n=1}^{N_s} \Omega_n$ where $\Omega_n$ is a smoothing domain for point at $\mathbf{x}_n$ and $N_s$ is the number of smoothing domains, as shown in Fig. 3. In constructing $\Omega_n$, we require that the interfaces of $\Omega_n$ do not share any portion of the discontinuous segments of the field function, they go across these discontinuous segments, and hence the field function is continuous on these interfaces of $\Omega_n$. We further assume that the strain in the smoothing domain is constant within each smoothing domain $\Omega_n$. Hence the

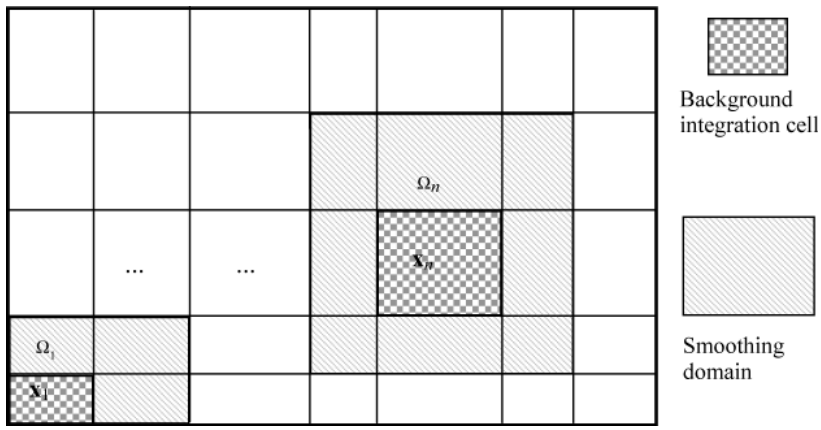


Fig. 2. Division of problem domain $\Omega$ into overlapping stationary smoothing domains $\Omega_n$ for $\mathbf{x}_n$. The integration cells are neither overlapping nor with gap.

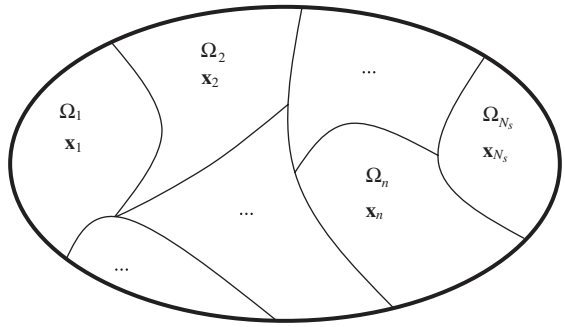


Fig. 3. Division of problem domain $\Omega$ into non-overlapping stationary smoothing domains $\Omega_n$ for $\mathbf{x}_n$. The smoothing domain is also used as basis for integration.

discretized bilinear form $\widehat{a}_D(w,v)$ using a stationary smoothing domain becomes

$$\widehat{a}_D(w,v) = \sum_{n=1}^{N_s} \left( \int_{\Omega_n} \frac{\partial v_i(\boldsymbol{\xi})}{\partial x_j} \widehat{W}(\mathbf{x}_n - \boldsymbol{\xi}) \mathrm{d}\boldsymbol{\xi} \right) C_{ijkl} \left( \int_{\Omega_n} \frac{\partial w_k(\boldsymbol{\xi})}{\partial x_l} \widehat{W}(\mathbf{x}_n - \boldsymbol{\xi}) \mathrm{d}\boldsymbol{\xi} \right),$$

$$= \sum_{n=1}^{N_s} A_n \, \widehat{\varepsilon}_n^T(v) \mathbf{C} \, \widehat{\varepsilon}_n \, (w) \tag{43}$$

where $\widehat{W}$ satisfies conditions (36)–(38) and it should be chosen for desired accuracy of integral representation. The simple summation is possible because $\Omega_n$ is constructed in such a way that $v$ and $w$ are continuous on these interfaces of $\Omega_n$. The integrals can be carried out using Eq. (32) for computing $\widehat{\varepsilon}$. It is clear that this bilinear form will still have basic properties, such as symmetry

$$\widehat{a}_D(w,v) = \widehat{a}_D(v,w), \quad \forall w, v \in \tilde{\mathbb{S}} \tag{44}$$

and positive definite, if the smoothing domain is properly constructed (see Sec. 5.6):

$$\widehat{a}_D(w,w) \geq 0, \quad \forall w \in \mathbb{S}, \quad \text{and} \quad \widehat{a}_D(w,w) = 0 \quad \text{if and only if } w = 0 \tag{45}$$

When the constant smoothing function Eq. (39) is used, we have

$$\bar{a}_D(w,v) = \sum_{n=1}^{N_s} \frac{1}{A_n} \left( \int_{\Omega_n} \frac{\partial v_i(\boldsymbol{\xi})}{\partial x_j} d\boldsymbol{\xi} \right) C_{ijkl} \left( \int_{\Omega_n} \frac{\partial w_k(\boldsymbol{\xi})}{\partial x_l} d\boldsymbol{\xi} \right) \tag{46}$$

In the implementation and coding, we use the following equivalent line-integral form:

$$\bar{a}_D(w,v) = \sum_{n=1}^{N_s} \frac{1}{A_n} \left( \int_{\Gamma_n} v_i n_j d\Gamma \right) \left( C_{ijkl} \int_{\Gamma_n} w_k n_l d\Gamma \right), \tag{47}$$

or

$$\bar{a}_D(w,v) = \sum_{n=1}^{N_n} A_n \bar{\boldsymbol{\varepsilon}}_n^T(v) \mathbf{C} \bar{\boldsymbol{\varepsilon}}_n(w) \tag{48}$$

where the *smoothed* strain $\bar{\boldsymbol{\varepsilon}}_n$ is can now computed using

$$\bar{\boldsymbol{\varepsilon}}_n(\mathbf{u}) = \frac{1}{A_n}\int_{\Omega_n} \varepsilon(\mathbf{x})d\Omega = \frac{1}{A_n}\int_{\Omega_n} \frac{\partial \upsilon_i(\boldsymbol{\xi})}{\partial x_j} d\boldsymbol{\xi} = \frac{1}{A_n}\int_{\Gamma_n} \mathbf{L}_n\mathbf{u}(\mathbf{x})d\Gamma. \tag{49}$$

### 5.5. *Smoothed Galerkin weakform solution*

We now discuss the solution of a weakform statement using the smoothed bilinear form. The node-based smoothed point interpolation method (NS-PIM) [Liu and Zhang (2005, 2008)] is one of the typical examples formulated using the smoothed bilinear form, which has a number of important properties that have been proven based on matrix formulation that is popular in mechanics community. It offers a very simple way to obtain an upper bound solution to the exact solution of a solid mechanics problem using a triangular mesh and PIM shape functions of different order and RPIM shape functions [Wang and Liu (2002)]. Here we first define the smoothed Galerkin weakform and then prove some of the important properties.

The smoothed Galerkin weakform solution $\widehat{u} \in \mathbb{G}_0^1$ satisfies

$$\widehat{a}_D(\widehat{u}, \upsilon) = f(\upsilon), \quad \forall\, \upsilon \in \mathbb{G}_0^1. \tag{50}$$

Note that here we make no changes to the linear functional, and the displacements are assumed in the same form as in Eq. (22) with shape functions properly constructed.

**Remark 5.6.** A smoothed Galerkin weak form Eq. (50) using smoothed strain over stationary smoothing domains is variationally consistent, if the solution as sought in $\mathbb{S}$.

**Proof.** To prove the variational consistence, one needs to examine the orthogonal condition [Simo and Hughes (1998)] that was defined over the problem domain. Because the strain field here is assumed constant in the stationary smoothing domains, and the integration over the entire problem domain is simply a summation of integrations over each of the smoothing domains. Therefore, the orthogonal condition becomes:

$$\int_{\Omega_n} \widehat{\boldsymbol{\varepsilon}}_n^T \mathbf{c}(\mathbf{L}_d\mathbf{u})\mathrm{d}\Omega = \int_{\Omega_n} \widehat{\boldsymbol{\varepsilon}}^T \mathbf{c}\, \widehat{\boldsymbol{\varepsilon}}\, \mathrm{d}\Omega \tag{51}$$

Since $\widehat{\boldsymbol{\varepsilon}}_n$ is constant in $\Omega_n$, and using the fact that

$$\int_{\Gamma_n} (\mathbf{L}_n\mathbf{u})\mathrm{d}\Gamma = \widehat{\boldsymbol{\varepsilon}}_n A_n \tag{52}$$

we immediately have

$$\int_{\Omega_n} \widehat{\boldsymbol{\varepsilon}}_n^T \mathbf{c}(\mathbf{L}_d\mathbf{u})\mathrm{d}\Omega = (\widehat{\boldsymbol{\varepsilon}}_n^T\mathbf{c}) \underbrace{\int_{\Gamma_n} (\mathbf{L}_n\mathbf{u})\mathrm{d}\Gamma}_{\widehat{\boldsymbol{\varepsilon}}_n A_n} = \widehat{\boldsymbol{\varepsilon}}_n^T \mathbf{c} \widehat{\boldsymbol{\varepsilon}}_n A_n = \int_{\Omega_n} \widehat{\boldsymbol{\varepsilon}}^T \mathbf{c} \widehat{\boldsymbol{\varepsilon}}\, \mathrm{d}\Omega \tag{53}$$

which is Eq. (51), and hence the orthogonal condition is satisfied for our smoothed train field using a stationary smoothing domain. □

### 5.6. *Properties of the smoothed bilinear form*

In this section, we discuss some of the properties of the smoothed bilinear forms. We will focus on discussion for functions in $H^1$ space, so that we can have a common comparison base.

**Remark 5.7.** *Convergence Property*: When $N_s \to \infty$ and all $\Omega_n \to 0$, $\widehat{W}$ becomes Delta functions and the integral representation will be exact. At such a limit $\widehat{a}_D(w, v) \to a(w, v)$.

**Theorem 5.1.** Softening effects: *For any* $w \in \mathbb{S}$ *and* $\widehat{W}$ *satisfies Eq.* (37) *for a set of stationary smoothing domains, we have*

$$\widehat{a}_D\ (w, w) \leq a_{\widehat{D}}(w, w), \tag{54}$$

*where*

$$a_{\widehat{D}}(w, w) = \sum_{n=1}^{N_s} \int_{\Omega_n} \left( \frac{\partial w_i}{\partial x_j} C_{ijkl} \frac{\partial w_k}{\partial x_l} \right) \widehat{W}(\mathbf{x}_n - \boldsymbol{\xi}) \mathrm{d}\boldsymbol{\xi}. \tag{55}$$

*In particular, when the constant smoothing function Eq.* (39) *is used in these stationary smoothing domains, we further have*

$$\bar{a}_D(w, w) \leq a(w, w). \tag{56}$$

**Proof.** Using Eq. (43), $\widehat{a}_D(w, w)$ can be written as

$$\widehat{a}_D(w, w) = \sum_{n=1}^{N_s} \left( \int_{\Omega_n} \frac{\partial w_i}{\partial x_j}\ \widehat{W}(\mathbf{x}_n - \boldsymbol{\xi}) \mathrm{d}\boldsymbol{\xi} \right) C_{ijkl} \left( \int_{\Omega_n} \frac{\partial w_k}{\partial x_l}\ \widehat{W}(\mathbf{x}_n - \boldsymbol{\xi}) \mathrm{d}\boldsymbol{\xi} \right). \tag{57}$$

To prove Eq. (54), we need only to prove

$$\left( \int_{\Omega_n} \frac{\partial w_i}{\partial x_j}\ \widehat{W}(\boldsymbol{\xi}) \mathrm{d}\boldsymbol{\xi} \right) C_{ijkl} \left( \int_{\Omega_n} \frac{\partial w_k}{\partial x_l}\ \widehat{W}(\boldsymbol{\xi}) \mathrm{d}\boldsymbol{\xi} \right) \leq \int_{\Omega_n} \frac{\partial w_i}{\partial x_j} \left( C_{ijkl} \frac{\partial w_k}{\partial x_l} \right) \widehat{W}(\boldsymbol{\xi}) \mathrm{d}\boldsymbol{\xi} \tag{58}$$

where $\widehat{W} = \widehat{W}(\mathbf{x}_n - \boldsymbol{\xi})$ is the smoothing function for $\Omega_n$ satisfying Eq. (37). We now discretize $\Omega_n$ into $n_q$ small subdomains: $\Omega_n = \bigcup_{q=1}^{n_q} \Omega_{n,q}$, and using the symmetry

property of $C_{ijkl}$, the term on left-hand side of Eq. (58) becomes:

$$\begin{aligned}
&\left(\int_{\Omega_n} \frac{\partial w_i}{\partial x_j}\, \widehat{W}(\boldsymbol{\xi})\mathrm{d}\boldsymbol{\xi}\right) C_{ijkl} \left(\int_{\Omega_n} \frac{\partial w_k}{\partial x_l}\, \widehat{W}(\boldsymbol{\xi})\mathrm{d}\boldsymbol{\xi}\right) \\
&= \lim_{n_q\to\infty} \left(\sum_{q=1}^{n_q} \left.\frac{\partial w_i}{\partial x_j}\right|_q \widehat{W}_q A_q\right) C_{ijkl} \left(\sum_{q=1}^{n_q} \left.\frac{\partial w_k}{\partial x_l}\right|_q \widehat{W}_q A_q\right) \\
&= \lim_{n_q\to\infty} \left( \begin{array}{l} \displaystyle\sum_{q=1}^{n_q} \widehat{W}_q^2 A_q^2 \left.\frac{\partial w_i}{\partial x_j}\right|_q C_{ijkl} \left.\frac{\partial w_k}{\partial x_l}\right|_q + 2\,\widehat{W}_1\widehat{W}_2\, A_1 A_2 \left.\frac{\partial w_i}{\partial x_j}\right|_1 C_{ijkl} \left.\frac{\partial w_k}{\partial x_l}\right|_2 \\ \qquad + \cdots + 2\,\widehat{W}_2\widehat{W}_3\, A_1 A_3 \left.\frac{\partial w_i}{\partial x_j}\right|_2 C_{ijkl} \left.\frac{\partial w_k}{\partial x_l}\right|_3 \\ \qquad + \cdots + 2\,\widehat{W}_{q-1}\widehat{W}_q\, A_{q-1} A_q \left.\frac{\partial w_i}{\partial x_j}\right|_{q-1} C_{ijkl} \left.\frac{\partial w_k}{\partial x_l}\right|_q \end{array} \right)
\end{aligned} \tag{59}$$

Using the triangular inequality, we have

$$2 \left.\frac{\partial w_i}{\partial x_j}\right|_q C_{ijkl} \left.\frac{\partial w_k}{\partial x_l}\right|_p \le \left.\frac{\partial w_i}{\partial x_j}\right|_q C_{ijkl} \left.\frac{\partial w_k}{\partial x_l}\right|_q + \left.\frac{\partial w_i}{\partial x_j}\right|_p C_{ijkl} \left.\frac{\partial w_k}{\partial x_l}\right|_p . \tag{60}$$

Substituting the above equation into Eq. (59) leads to:

$$\begin{aligned}
&\left(\int_{\Omega_n} \frac{\partial w_i}{\partial x_j}\, \widehat{W}(\boldsymbol{\xi})\mathrm{d}\boldsymbol{\xi}\right) C_{ijkl} \left(\int_{\Omega_n} \frac{\partial w_k}{\partial x_l}\, \widehat{W}(\boldsymbol{\xi})\mathrm{d}\boldsymbol{\xi}\right) \\
&\quad \le \lim_{n_q\to\infty} \left( \left(\sum_{q=1}^{n_q} \widehat{W}_q A_q\right) \sum_{q=1}^{n_q} \widehat{W}_q A_q \left.\frac{\partial w_i}{\partial x_j}\right|_q C_{ijkl} \left.\frac{\partial w_k}{\partial x_l}\right|_q \right) \\
&\quad = \int_{\Omega_n} \left(\frac{\partial w_i}{\partial x_j} C_{ijkl} \frac{\partial w_k}{\partial x_l}\right) \widehat{W}(\boldsymbol{\xi})\mathrm{d}\boldsymbol{\xi}
\end{aligned} \tag{61}$$

which gives Eq. (58) and hence (54). In the above derivation, we used Eq. (35):

$$\lim_{n_q\to\infty} \sum_{q=1}^{n_q} \widehat{W}_q A_q = \int_{\Omega_n} \widehat{W}(\boldsymbol{\xi})\mathrm{d}\boldsymbol{\xi} = 1 \tag{62}$$

and

$$\lim_{n_q\to\infty} \sum_{q=1}^{n_q} \widehat{W}_q A_q \left.\frac{\partial w_i}{\partial x_j}\right|_q C_{ijkl} \left.\frac{\partial w_k}{\partial x_l}\right|_q = \int_{\Omega_n} \left(\frac{\partial w_i}{\partial x_j} C_{ijkl} \frac{\partial w_k}{\partial x_l}\right) \widehat{W}(\boldsymbol{\xi})\mathrm{d}\boldsymbol{\xi}. \tag{63}$$

Substituting Eq. (39) into Eq. (58), we further have

$$\underbrace{\frac{1}{A_n} \left(\int_{\Omega_n} \frac{\partial w_i}{\partial x_j} d\Omega\right) C_{ijkl} \left(\int_{\Omega_n} \frac{\partial w_k}{\partial x_l} d\Omega\right)}_{\widehat{a}_D(w,w)} \le \underbrace{\int_{\Omega_n} \frac{\partial w_i}{\partial x_j} \left(C_{ijkl} \frac{\partial w_k}{\partial x_l}\right) d\Omega}_{a(w,w)} \tag{64}$$

which leads clearly to Eq. (56). □

Theorem 5.1 implies that the smoothing operation provides "softening" effect to the system. Hence a model established based on the smoothed Galerkin projection will be "softer" than that based on the Galerkin projection.

**Theorem 5.2.** Monotonic convergence property: *For any* $w \in \mathbb{S}$, *in a given division* $D_1$ *of domain* $\Omega$ *into a set of smoothing domains* $\Omega = \bigcup_{n=1}^{N_s} \Omega_n$, *if a new division* $D_2$ *is created by sub-dividing a smoothing domain in* $D_1$ *into* $n_{sd}$ *sub-smoothing-domains*: $\Omega_n = \bigcup_{i=1}^{n_{sd}} \Omega_{n,i}$, *then the following inequality stands*

$$\bar{a}_{D_1}(w, w) \leq \bar{a}_{D_2}(w, w). \tag{65}$$

**Proof.** Note that the difference between $\bar{a}_{D_1}(w, w)$ and $\bar{a}_{D_2}(w, w)$ is only at the $n$th smoothing domain $\Omega_n$. Therefore, we need only compare the contributions from $\Omega_n$ and the sub-divided $\bigcup_{i=1}^{n_{sd}} \Omega_{n,i}$. The sub-division gives

$$\int_{\Omega_n} \frac{\partial w_i}{\partial x_j} d\Omega = \sum_{q}^{n_{sd}} \int_{\Omega_{n,q}} \frac{\partial w_i}{\partial x_j} d\Omega. \tag{66}$$

Therefore, we have

$$\begin{aligned} &\frac{1}{A_n} \left( \int_{\Omega_n} \frac{\partial w_i}{\partial x_j} d\Omega \right) C_{ijkl} \left( \int_{\Omega_n} \frac{\partial w_k}{\partial x_l} d\Omega \right) \\ &\quad = \frac{1}{A_n} \left( \sum_{q=1}^{n_{sd}} \int_{\Omega_{n,q}} \frac{\partial w_i}{\partial x_j} d\Omega \right) C_{ijkl} \left( \sum_{q=1}^{n_{sd}} \int_{\Omega_{n,q}} \frac{\partial w_k}{\partial x_l} d\Omega \right) \\ &\quad \leq \frac{1}{A_n} \sum_{q=1}^{n_{sd}} \left[ \left( \int_{\Omega_{n,q}} \frac{\partial w_i}{\partial x_j} d\Omega \right) C_{ijkl} \left( \int_{\Omega_{n,q}} \frac{\partial w_k}{\partial x_l} d\Omega \right) \right]. \end{aligned} \tag{67}$$

In the above equation we used the *triangular inequality* of norms: sum of energy norm of functions is no-less than the norm of the summed functions. Therefore, Eq. (65) stands. □

Theorem 5.2 implies that the "softening" effect provided by the smoothed Galerkin projection will be monotonically reduced with the increase of the number of smoothing domain in a nested manner. Note that at the extreme case, we can perform the smoothing operation over the entire domain $\Omega_n = \Omega_1 = \Omega_1$, in this case we shall have the following corollary as a special case of Theorem 5.2.

**Theorem 5.3.** Upper bound to the exact solution: *The strain energy of the exact solution* $u$ *is no-larger than that of the smoothed Galerkin weakform solution* $\bar{u} \in \mathbb{S}$ *when the smoothing operation is performed on the solution* $u \in \mathbb{S}$

$$a(u, u) \leq \bar{a}_D(\bar{u}, \bar{u}). \tag{68}$$

**Proof.** From Eqs. (20) and (50), we have

$$a(u,\upsilon) = \bar{a}_D(\bar{u},\upsilon), \quad \forall\, \upsilon \in \mathbb{S}. \tag{69}$$

Let $\upsilon = u$ (at the minimum of the total potential energy of the Galerkin model), we should have

$$a(u,u) = \bar{a}_D(\bar{u},u). \tag{70}$$

On the other hand, if we let $\upsilon = \bar{u}$ (at the minimum of the total potential energy of the smoothed Galerkin model), we should have

$$a(u,\bar{u}) = \bar{a}_D(\bar{u},\bar{u}) \tag{71}$$

We next examine

$$\underbrace{\bar{a}_D(\bar{u}-u,\bar{u}-u)}_{\geq 0} = \bar{a}_D(\bar{u},\bar{u}) - 2\underbrace{\bar{a}_D(u,\bar{u})}_{=a(u,u)} + \bar{a}_D(u,u) \geq 0 \tag{72}$$

Using Eq. (71), the positivity and symmetry property of $\bar{a}(,)$, we have

$$\underbrace{[a(u,u) - \bar{a}_D(u,u)]}_{\geq 0} + a(u,u) \leq \bar{a}_D(\bar{u},\bar{u}) \tag{73}$$

With the help of Theorem 5.1, we have $[a(u,u) - \bar{a}_D(u,u)] \geq 0$ which gives the inequality (68). □

### 5.7. *On number of smoothing domains*

When stationary smoothing domains are used for establishing a smoothed Galerkin model, the minimum number of smoothing domains needs to be determined based on the number of filed nodes used. The consideration should be: the total number of equations that are sampled from all the smoothing domains $N_s$ should be no-less than the total number of unknowns in the model $N_u$. For example, for a 2D solid mechanics problem model with $n_t$ (unconstrained) nodes used for displacement field construction, the total number of unknowns in the model should be $N_u = 2n_t$, because one node carries two unknowns (displacement components in $x$ and $y$ directions). The total number of equations that can be sampled from all the smoothing domains should be $3N_s$, because one smoothing domain gives three independent equations (three strain components). Therefore, $N_s = 2n_t/3$. Based on the same consideration, we have:

**Remark 5.8.** Minimum number of smoothing domains: when stationary smoothing domains are used to create a smoothed Galerkin model, the minimum number of smoothing domains is given in Table 1.

Violation of Table 1, the discretized system equations established using the smoothed Galerkin weak form will be singular, and no unique solution will be

Table 1. Minimum number of smoothing domains $N_s^{\min}$ for solid mechanics problems.

| Dimension of the Problem | Minimum Number of Smoothing Domains |
|---|---|
| 1D | $N_s^{\min} = n_t$ |
| 2D | $N_s^{\min} = 2n_t/3$ |
| 3D | $N_s^{\min} = 3n_t/6{=}n_t/2$ |

obtained. The use of more smoothing domains does not necessarily guarantee a nonsingular set of system equations, because it depends also on how the division of the smoothing domains is performed. As long as the number of smoothing domains is concerned, a finer division of smoothing domains generally leads to a stiffer model (see Theorem 5.2). In this regards, to obtain an upper bound solution, one needs to create a relatively softer model, and hence should use a smaller number of smoothing domains, as it is done in the LC-PIM. On the other hand, when we want to remove spurious modes and to have temporal stability, we should use more smoothing domains, as we do in the ES-PIM.

### 5.8. *Node-based smoothed point interpolation method*

Theorem 5.3 provides very powerful means to develop numerical methods that can produce upper bound solution to the exact solution in strain energy norm. However, the exact solution space is not usually attainable or we do not need any numerical method. Hence we have to perform the smoothing operation based on discrete solution space that is attainable. The use of the functions created using point interpolation produces the so-called node-based smoothed point interpolation method (NS-PIM).

The NS-PIM [Liu and Zhang (2005, 2008)] and is a typical example using the smoothed bilinear form, and offers a very simple and general way to obtain an upper bound solution to the exact solution of a solid mechanics problem. As a mesh free method, the shape functions are generated using local support domains that are generally overlapping, and PIM shape functions of different order and RPIM shape functions are used. Any of the PIM and RPIM shape functions can also be used without worrying about the compatibility in the NS-PIM procedure, due to the use of the generalized smoothed bilinear form. The NS-PIM generally uses a triangular mesh for guiding the node selection for the interpolation and for the smoothing domain construction, because a triangular mesh can be generated automatically for complicated problem domains.

In the NS-PIM the smoothing domains are node-based. The problem domain $\Omega$ is meshed with $N_e$ elements of, say, triangles with total of $N_n$ nodes as we do in the FEM procedure. Based on these triangular elements, the domain is then divided into $N_s$ smoothing domains $\Omega = \bigcup_{n=1}^{N_s} \Omega_n$, and each $\Omega_n$ contains a node and covers

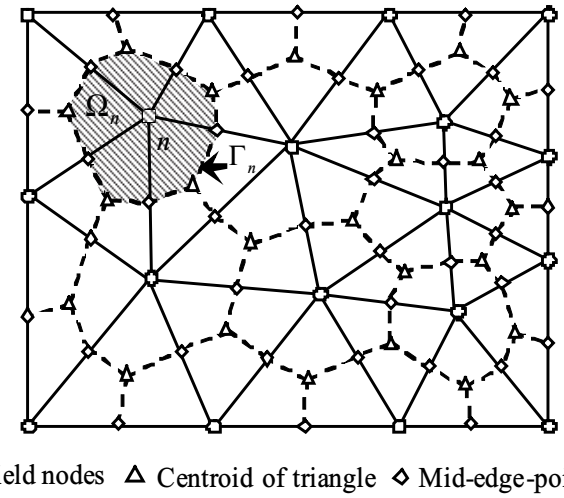


Fig. 4. NS-PIM formulation: Triangular elements (bounded by solid lines) and the non-overlapping stationary smoothing domain $\Omega_n$ (bounded by dashed lines $\Gamma_n$) for node $n$ created by connecting the centroids with the mid-edge-points of the surrounding triangles of a node. The smoothing operation is performed over the entire node-based smoothing cell. The integration is also based on these smoothing cells.

portions of elements sharing the node, as shown Fig. 4. Therefore, in this case we have $N_s = N_n$. The smoothed Galerkin weakform solution $\bar{u} \in \mathbb{G}_0^1$ satisfies

$$\bar{a}_D(\bar{u}, v) = f(v), \quad \forall v \in \mathbb{G}_0^1, \tag{74}$$

where the subscript "$D$" denotes the division of the problem domain into smoothing domains based on the finite element mesh. Equation (74) is in fact the so-called generalized Galerkin weakform with variational consistence, if none of the $\Omega_n$ is further divided. In the field function approximation, the PIM or RPIM shape functions are used in the following interpolation,

$$\bar{u}(\mathbf{x}) = \sum_{i=1}^{N_n} \bar{d}_i \varphi_i(\mathbf{x}), \tag{75}$$

where $\bar{d}_i$ is a nodal displacement, and $\varphi_i$ is nodal shape function that are created using a point interpolation method. In the NS-PIM, a simple scheme for local supporting node selection is suggested based on the background triangular cells for shape function construction. The background triangular cells are classified into two groups: interior cells and edge cells. An interior cell is a cell that has no edge on the boundary of the problem domain, and an edge cell is a cell that has at least one edge on the boundary of the problem domain. The node selection scheme is then based on the order of the interpolation to be used. For linear NS-PIM where linear interpolation is used, we simple use three nodes of the home cell that houses the point of interest (usually the quadrature sampling point). For quadratic NS-PIM,

we quadratic interpolations for interior cells and linear interpolations for edge cells. Three nodes located at the vertices of the home cell, and the other three nodes located at the remote vertices of the three neighboring cells. Conformability can be ensured by the later implementation of nodal integrations with smoothing operation on strains.

We then substitute Eq. (75) into (74), and set $\varphi_i, i = 1, \ldots, N_n$, as the test function $v$, we have the following discrete set of $\aleph$ equations.

$$\sum_{j=1}^{N_n} \bar{a}_D(\varphi_j, \varphi_i)\bar{d}_j = f(\varphi_i), \quad i = 1, \ldots, N_n \tag{76}$$

which can be written in the matrix form of

$$\bar{\mathbf{K}}\bar{\mathbf{d}} = \tilde{\mathbf{f}}, \tag{77}$$

where $\bar{\mathbf{K}}$ is the NS-PIM stiffness matrix with entries of $\bar{K}_{ij} = \bar{a}_D(\varphi_j, \varphi_i)$, $1 \leq i$, $j \leq N_n$, $\bar{\mathbf{d}}$ is the vector of nodal displacements $\bar{d}_i$, and $\tilde{\mathbf{f}}$ is the vector with entries of $f(\varphi_i)$, which is the same as that in the FEM.

The NS-PIM has the same properties presented in Sec. 5.4, as those properties are derived for any division of domain into smoothing domains. Based on Theorem 5.3, we further have the following theorem.

**Theorem 5.4.** Upper bound to the FEM solution: *When the solution is sought in the finite element solution space, the strain energy of the NS-PIM solution $\bar{u}$ is no-less than that of the FEM solution $\tilde{u}$*:

$$a(\tilde{u}, \tilde{u}) \leq \bar{a}_D(\bar{u}, \bar{u}). \tag{78}$$

The proof of this theorem follows exactly the procedure of Theorem 5.3, but consider the FEM space $\tilde{\mathbb{S}}$.

Theorem 5.4 does not tell whether a NS-PIM solution will be the upper bound of the exact solution. To answer this, we have the following useful theorem.

**Theorem 5.5.** Upper bound to the exact solution*: The strain energy of the NS-PIM solution $\bar{u}$ is no-less than that of the exact solution $u$*:

$$a(u, u) \leq \bar{a}_D(\bar{u}, \bar{u}), \tag{79}$$

*with exception of a few trivial cases of insufficient smoothing operations.*

Precise proof of Theorem 5.5 is difficult, because the conditions for Eq. (79) are difficult to give in a precise manner. An explanation on Theorem 5.5 based on the so-called "the battle between the softening and hardening effects" can be found in Liu and Zhang (2008). We have found Eq. (79) is not true for problems of insufficient smoothing operations. One such a counter example is when only one linear element is used in a NS-PIM model. In such a case, the node-based smoothing operation has no effects and the NS-PIM solution is the same as that of FEM that is a lower bound of the exact solution. Fortunately, when the element number increases, more

nodes are shared by more than one elements, hence the smoothing takes bigger effects resulting in smoothed strains for the nodes, which produces upper bound solution in energy norm. Many cases have been studied using NS-PIM, and they all confirm Eq. (79), including the cases studied using LC-RPIM where the RPIM shape functions are used. Therefore, Theorem 5.5 is of practical importance.

### 5.9. *Smoothed finite element method (SFEM)*

The other method that uses the smoothed Galerkin weakform is the so-called smoothed finite element method (SFEM), where the solution is usually sought in an $H^1$ space. In the SFEM, the smoothing domains are constructed based on a FEM mesh, the SFEM model can be established using the same FEM mesh, and the smoothing domains (or cells) are constructed based on elements. The physical domain $\Omega$ is first meshed with $N_e$ elements of say, quadrilaterals as we do in the FEM procedure, and an element is further divided to form a number of smoothing domains/cells, as shown in Fig. 5, which gives a total of $N_s$ smoothing domains, and $\Omega = \bigcup_{n=1}^{N_s} \Omega_n$. In this case we shall have $N_s \geq N_e$.

The formulation of SFEM is largely similar to that of NS-PIM, but it uses the FEM shape functions created based on elements and the element-based smoothing domains are used. Therefore, it requires little change to the FEM codes. Note that in the SFEM formulation, n-sided polygonal elements can be used. Many other good properties of SFEM have been found such as resilience to the element mesh distortion accurate in stress solution, etc.

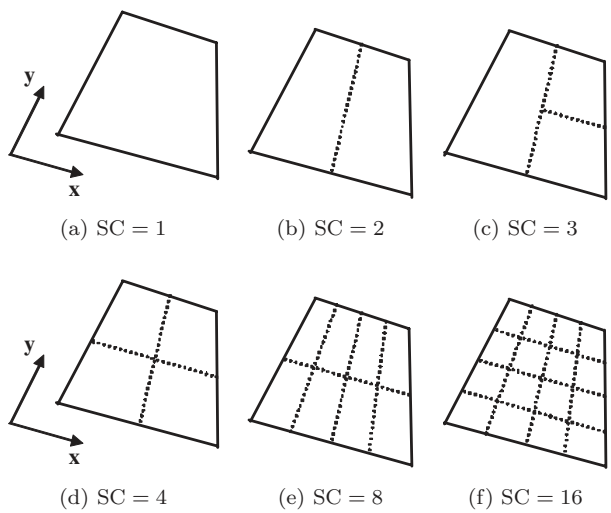


(a) SC = 1 (b) SC = 2 (c) SC = 3

(d) SC = 4 (e) SC = 8 (f) SC = 16

Fig. 5. SFEM formulation: Division of an quadrilateral element in a FEM mesh into smoothing domains/cells (SC). (a) Only one smoothing cell is used for the element (SC = 1). (b) Two smoothing cells are used for the element (SC = 2), and so on. The smoothing operation is then performed for each of these cells.

Theorem 5.4 stands also for the SFEM, but Theorem 5.5 may or may not stand. Studies have shown that the validity of Theorem 5.5 will be problem dependent. For a class of problems called *overestimation* problems, SFEM can produce upper bound solution to the exact solution, when a small number of smoothing cells is used for the elements. For many problems, the SFEM based on linear elements will not be able to produce upper bound solutions to the exact solution.

Note that the equality in Eq. (79) can be achieved when we use linear triangular elements. In such a case, the smoothing operation to the elements has no effect at all, regardless how many smoothing cells is used in an element, and hence the SFEM produces the same solution as the FEM. This is a typical case that violates Theorem 5.5, regardless how many elements are used.

### 5.10. *Node-based smoothed finite element method (N-SFEM)*

Based on the idea of the smoothed finite element method (SFEM) and the NS-PIM formulation, a node-based SFEM or N-SFEM has been proposed recently, and applied to n-sided polygonal elements. In the N-SFEM, the smoothed Galerkin weakform is used and the smoothing domains are node-based, as shown in Fig. 6. The problem domain $\Omega$ is meshed with $N_e$ elements of n-sides with a total of $N_n$

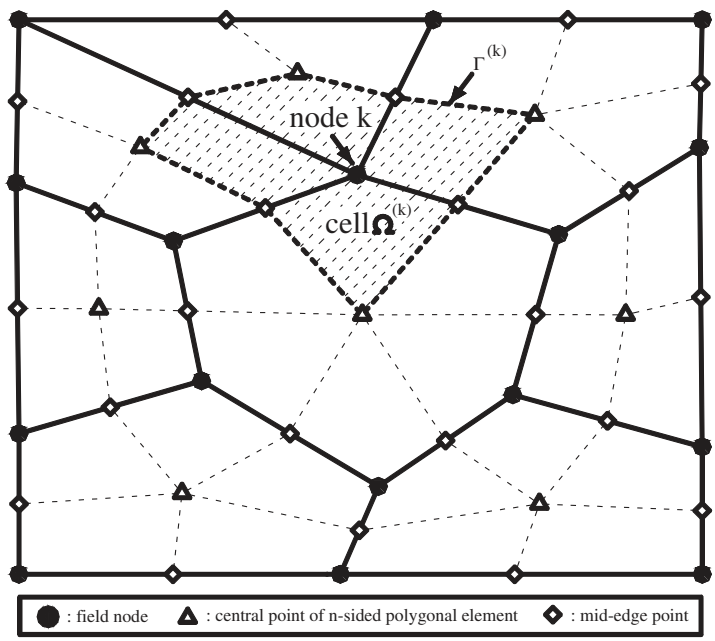


Fig. 6. N-SFEM: n-sided polygonal elements (bounded by solid edges) and the non-overlapping stationary smoothing cells/domains (shaded area) associated with node $k$. The smoothing operation is performed over the entire node-based smoothing cell.

nodes as we do in the FEM procedure and the solution is usually sought in an $H'$ space. Then $N_s$ smoothing domains are formed with each $\Omega_n$ contains a node and covers the portions of the elements sharing this node. Therefore, in this case $N_s = N_n$.

The formulation of the N-SFEM is similar to that of the NS-PIM except that FEM shape functions created based on elements are used. Both Theorems 5.4 and 5.5 hold for N-SFEM. Therefore, N-SFEM is also a powerful method that produces upper bound solutions to the exact solution. Many cases have been studied using N-SFEM and they all confirm Eq. (80). Therefore, Theorem 5.5 is of practical importance for N-SFEM. Note also that the upper bound property of N-SFEM exists for n-sided elements including the triangular elements. It offers an excellent method for accurate solutions with bounds using triangular element mesh, and adaptive analysis procedures can be easily implemented.

### 5.11. *The battle of softening and stiffening effects*

In the above analysis, we noted that the NS-PIM and N-SFEM can provide an upper bound for the exact solution in energy norm for structural mechanics problems. However, the SFEM does not necessarily provide such an upper bound solution for all the problems. What is the reason behind this discrepancy? The argument of "battle of softening and stiffening effects" was first put forward by Liu *et al.* provides an insightful understanding on this matter. We now discuss more about this matter in a unified manner based on the new theorems that we established in this paper.

Based on Theorem 5.1, we know that the smoothed bilinear form produces a model that is "*softer*" than the actual solids or structure, so that the strain energy obtained by NS-PIM (or N-SFEM or SFEM) is "larger" than that of the exact solution, as long as the smoothing operation is preferred to the exact solution. This fact is coined as *softening effect*. This softening effect also exists when the bilinear form applies to an assumed solution space, meaning that the smoothed bilinear form produces a model that is "*softer*" than the numerical model of the actual solids or structure. Therefore, the strain energy obtained by NS-PIM (or N-SFEM) is "larger" than that of the FEM solution, as stated in Theorem 5.4.

On the other hand, the FEM approximation creates a model that is "stiffer" than the actual solid or structure and resulting in an underestimation of strain energy as stated in Remark 4.1. This is called the "*stiffening effect*", and is caused by the assumed displacement filed using the FEM shape functions in a conforming/fully-compatible model. The same effect will also occur when PIM shape functions are used as long as the formulation is conforming as in the NS-PIM.

The battle between the softening and stiffening effects will determine whether a NS-PIM (or N-SFEM or SFEM) model can in fact provide an upper bound solution to the problem.

The softening effect depends on the following situations in a NS-PIM (or N-SFEM or E-SFEM or SFEM) model.

- Significantly larger smoothing effects are gained when the smoothing domain is chosen across the lines of strain discontinuity, such as the interfaces of the elements or background cells. NS-PIM and N-SFEM models use smoothing domains cover multiple strain discontinuity lines and hence achieved sufficient smoothing effects to obtain upper bound solutions. The E-SFEM models use smoothing domains covers one strain discontinuity line per domain to gain a moderate smoothing effect for ultra-accurate solutions.
- For the case of NS-PIM and N-SFEM, the number of elements that connected to a node of a smoothing domain: The more the elements, the larger the smoothing effects. As shown in Fig. 4. At node $n$, there are five elements connected, and at the corner node $q$, however, only two elements are connected. In an extreme case, if element-based smoothing is performed ($\Omega_n$ is further divided to five sub-domains: each for an element and the smoothing is performed based on the sub-domains) and linear shape functions are used, there will be no softening effect at all. In this case, the NS-PIM and FEM gives naturally the same results, and the NS-PIM will not provide an upper bound, but a lower bound solution. When higher order shape functions are used as in the SFEM where bilinear shape functions are used and in the NS-PIM case where the 2nd order shape functions are used, an element-based smoothing will still have some softening effects, but it is very much smaller compared to the node-based smoothing. In this kind of cases, the model may or may not be able to produce the exact upper bound solution, as we observed in the SFEM.
- The number of nodes being smoothed. In NS-PIM (or N-SFEM), one does not have to perform the smoothing operation for all the nodes. If the smoothing is selectively performed, there will still be some smoothing effects and the general properties discussed in Sec. 5.4 will still hold, but the softening effect will propositionally depend on the number of nodes participated in the smoothing operation.
- In the case of SFEM, the elements are further sub-divided into smoothing cells. Therefore, the more the sub-division, the less the softening effects. Therefore, for an SFEM model producing an upper bound solution, one must use as small number of sub-division as possible.
- The number of nodes used in the problem domain or density of the background cells. When a small number of nodes are used, the displacements approximated using the PIM shape functions in a smoothing domain deviates far from the exact solution, resulting in a heavy smoothing to the strain field, and hence a strong softening effect. On the other hand, when a large number of nodes are used, the displacements approximated using the PIM shape functions in a smoothing domain is more close to the exact solution, resulting less smoothing effects, and hence less softening effect. At the extreme of infinitely small elements are used,

the smoothing effects will diminish and the NS-PIM solution (also the FEM solution) will approach to the exact solution. Remark 4.2 and Remark 5.9 provide theoretical supports to this claim.

The *stiffening effect* depends on the following situations in a NS-PIM (or N-SFEM or SFEM) model.

- The order of the PIM (or FEM) shape functions used in the displacement approximation. When high order shape functions are used, the displacements approximated using these shape functions in a smoothing domain are closer to the exact solution of displacements, which reduces the stiffening effect, and vice versa.
- The number of nodes used in the problem domain. When a small number of nodes are used, the displacements approximated using the PIM (or FEM) shape functions in a smoothing domain deviates far from the exact solution, the stiffening effect is therefore large, and vice verse. At the extreme of infinitely small elements are used, the stiffening effects will diminish and the NS-PIM solution (also the FEM solution) will approach to the exact solution.

Generally, the softening effect provided by the smoothing in a NS-PIM (or N-SFEM) model is more significant than the stiffening effects. This is because the smoothing is a zero order approximation that is lower than the at least first order approximation of the displacement resulting in the stiffening effect. Therefore, the NS-PIM (or N-SFEM) always produces an upper bound solution except a few trivial cases such as:

- Only one element is used. In this case, only element participates in smoothing, which should not have any smoothing effects, and hence the solutions of NS-PIM (or N-SFEM) and FEM are the same, and NS-PIM (or N-SFEM) gives a lower bound solution.
- Too few elements are used resulting in insufficient smoothing effect.

In the numerical study, it has found that NS-PIM (or N-SFEM) can produce upper bound solutions for all the problems we have studied, except the very special case mentioned above.

### 5.12. *Issues on spurious modes*

It is well-known that FEM model based on the complementary energy principles can also produce upper bound solutions. Such a model is much more difficult to establish, and will have the so-called spurious modes: modes that require still-some but much-less energy to excite. These modes look quite similar to the well-known hour-class modes in FEM model with reduced integration. The presence of these kinds of modes will affect the solution for dynamic problems, if a direct-integration-technique is used for the time matching.

Methods established using the present bilinear form may or may not have such a phenomenon of spurious modes. We have observed spurious modes in NS-PIM,

and the N-SFEM, but not in SFEM (when SC $\geq 4$). It is the author's predication that *when a numerical model produces upper bound* (*in strain energy*) *solution for static problems*, *the model will have spurious modes for dynamic problems*. Therefore, lower bound method is preferred for dynamic problems using direct-integration techniques, because there will be no spurious modes (if fully-integrated). Note that the spurious nodes appear only as higher modes, and the more nodes are used in the (say NS-PIM) model, the higher the spurious modes. At the fine limit, they disappear according to Remark 5.9. Therefore, when an upper bound method is used for dynamic problems, one may need to use techniques like the mode superimposition method for time integration, so that the higher modes can be excluded. When one has to use a direct-integration-method, some kind of stabilization technique may be needed. A very simple way to remove the spurious modes is using the E-SFEM where the smoothing domains are created based on the edges of the cells. The E-SFEM is briefed in the next section.

Note that the upper bound methods like NS-PIM and the N-SFEM has no stability problem at all for static problems, as proven in [Liu and Zhang (2008)]. In fact their equation systems are very stable and much better conditioned compared to the lower bound methods such as the FEM, and hence much more resilient to mesh distortion and accepts all type of element including triangular types of elements.

### 5.13. *Edge-based smoothed finite element method (E-SFEM)*

Based on the idea of the smoothed finite element method (SFEM) and the NS-PIM formulation, and the N-SFEM, an edge-based SFEM or (E-SFEM) has been proposed recently for general n-sided elements [Liu, Nguyen and Lam (2008a)]. In the E-SFEM, the smoothed Galerkin weakform is also used and the procedure is almost the same as the N-SFEM, except that the smoothing domains are created based on edges of the elements, as shown in Fig. 6. The E-SFEM was devised to remove the spurious modes observed in N-SFEM. This simple change of smoothing domain has successfully solved the spurious mode problem and produces very accurate results as shown in the next section.

## 6. Numerical Examples

We now present two numerical examples to examine the properties discussed in Sec. 5. We will focus on the upper bound properties due to its importance in obtaining certified solutions.

### 6.1. *Cantilever loaded at the end*

A cantilever of length $L$ and height $D$ subjected to a parabolic traction at the free end as shown in Fig. 8 is studied here to show these properties of the methods developed using the bilinear form. The cantilever is assumed to have a unit thickness

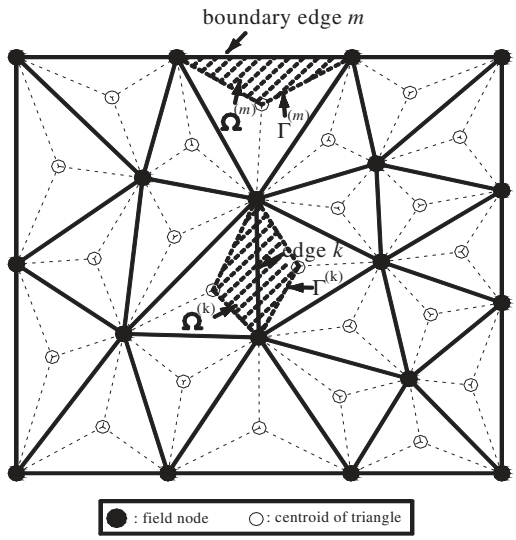


Fig. 7. E-SFEM formulation: Triangular elements (bounded by solid lines) and the smoothing domain $\Omega$ (bounded by dashed lines $\Gamma$) created by sequentially connecting the centroids of the surrounding triangles of an edge with the nodes on the edge. The smoothing operation is performed over the entire edge-based smoothing cell, or equivalently over the two triangles areas shearing the edge. The integration is performed based on the shaded smoothing domains.

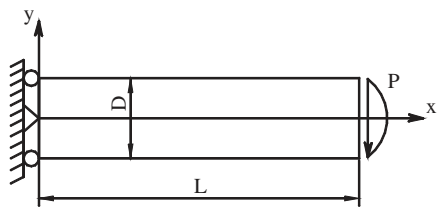


Fig. 8. Cantilever loaded at the end.

so that plane stress condition is valid. The analytical solution is available and can be found in a textbook by Timoshenko and Goodier [1970].

$$\begin{aligned} u_x &= \frac{Py}{6EI}\left[(6L-3x)x+(2+\nu)\left(y^2-\frac{D^2}{4}\right)\right] \\ u_y &= -\frac{P}{6EI}\left[3\nu y^2(L-x)+(4+5\nu)\frac{D^2x}{4}+(3L-x)x^2\right], \end{aligned} \tag{80}$$

where the moment of inertia $I$ for a beam with rectangular cross section and unit thickness is given by $I=\frac{D^3}{12}$.

The stresses corresponding to the displacements Eq. (80) are

$$\sigma_{xx}(x,y) = \frac{P(L-x)y}{I}; \quad \sigma_{yy}(x,y) = 0; \quad \tau_{xy}(x,y) = -\frac{P}{2I}\left(\frac{D^2}{4} - y^2\right). \tag{81}$$

The related parameters are taken as $E = 3.0 \times 10^7\,\text{Pa}$, $\nu = 0.3$, $D = 12\,\text{m}$, $L = 48\,\text{m}$ and $P = 1000\,\text{N}$. In the computations, the nodes on the left boundary are constrained using the exact displacements obtained from Eq. (80) and the loading on the right boundary uses the distributed parabolic shear stresses in Eq. (81).

We first use the SFEM with quadrilateral elements to perform the analysis with two smoothing cells in each element. The numerical strain energies have been plotted against the degrees of freedom (DOFs) in Fig. 9 with the FEM solution obtained using the same mesh. It is seen that the SFEM produces upper bound solution for this problem, while the FEM produces the lower bound solution.

We next use the N-SFEM and the E-SFEM to solve this problem. In general, both N-SFEM and E-SFEM can use n-sided polygonal elements of any order. Here we use triangular elements to perform the analysis with one smoothing cell/domain for each node for convenience of comparison. The numerical strain energies have been plotted against the DOFs in Fig. 10 with the FEM solution obtained using the same mesh and the same set of nodes. It is found that the N-SFEM can also produce upper bound solution for this problem. Note that when linear triangular elements are used, the results of the N-SFEM are the same as that in [Dohrmann *et al.* (2000)]. It is also found that the E-SFEM produces ultra accurate results

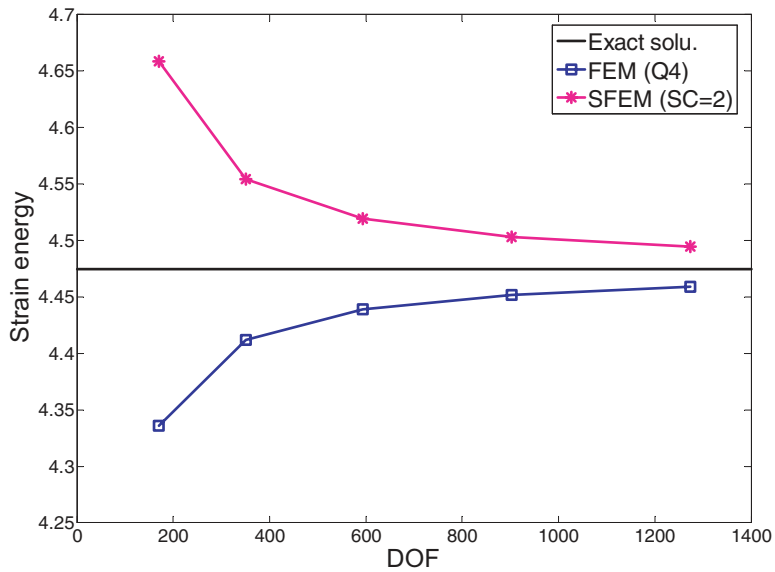


Fig. 9. Solutions for the cantilever beam obtained using FEM, SFEM with two smoothing cells in an element and the same triangular mesh in comparison with the exact solution.

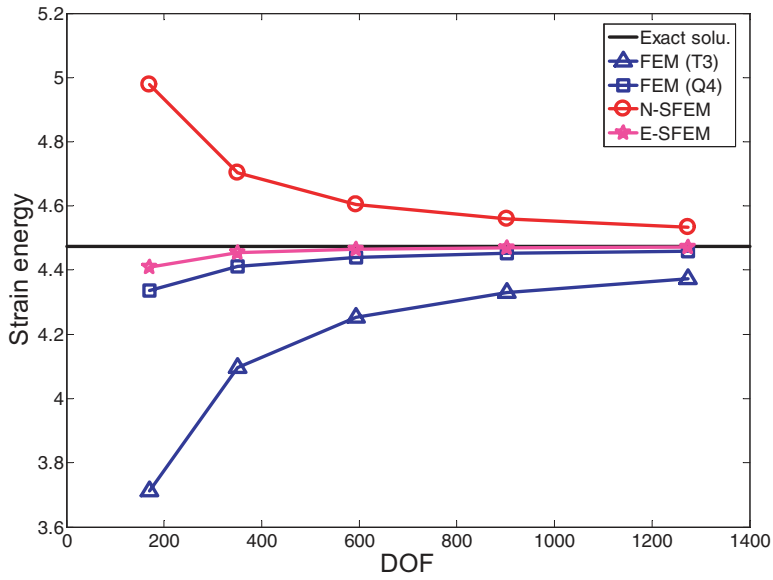


Fig. 10. Solutions for the cantilever beam obtained using FEM, N-SFEM, E-SFEM and the same triangular mesh in comparison with the exact solution.

that is even more accurate that the FEM solution using quadrilateral elements as shown in Fig. 10. In addition, it is seen that the E-SFEM is a lower bound solution, and hence will not produce any spurious modes. All these are achieved by simply choosing different smoothing cells/domains.

We now use the NS-PIM with triangular elements to perform the same analysis with one smoothing cell/domain for each node. The numerical strain energies have been plotted against the DOFs in Fig. 11 with the FEM solution obtained using the same mesh and the same set of nodes. It is found that the NS-PIM can also produce upper bound solution for this problem. Note that when linear interpolation is used the NS-PIM and N-SFEM-T3 will give the same results. However, NS-PIM can use higher order interpolation based on the same mesh and nodes. For the case of quadratic NS-PIM shown in Fig. 11, 6 nodes are used in the interpolation in an overlapping manner, and same triangular mesh of some number of nodes can be used. For the use of arbitrary number of nodes in the interpolation, reader can refer to [Liu *et al.* (2006)].

In summary, for cantilever beam problem, all these three methods produce upper bound solutions.

### 6.2. *Infinite plate with a circular hole*

We now perform the same study as in the previous section for an infinite plate with a circular hole subjected to a unidirectional tensile load of $\sigma = 1.0\,\mathrm{N/m}$ at

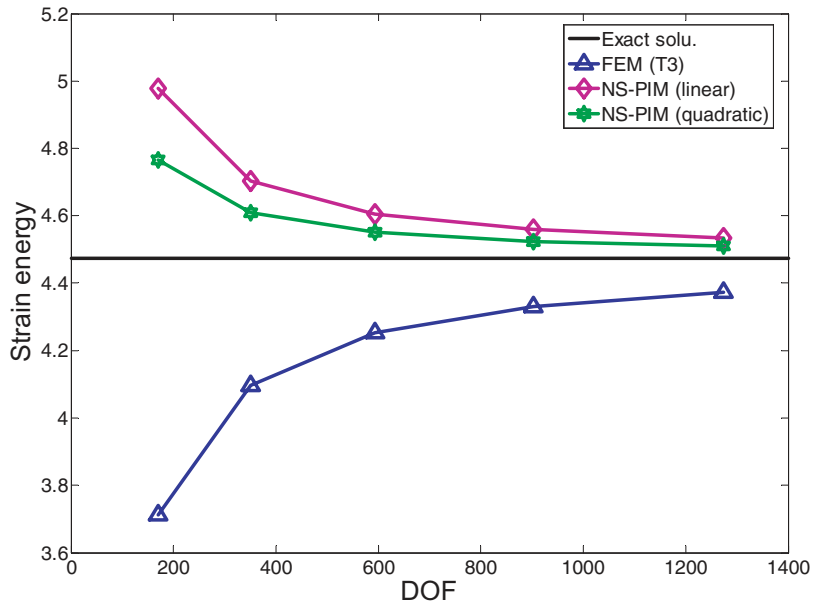


Fig. 11. Solutions for the cantilever beam obtained using FEM, NS-PIM and the same triangular mesh in comparison with the exact solution. For the case of quadratic NS-PIM, 6 nodes are used in the interpolation in an overlapping manner, and hence same triangular mesh of some number of nodes can be used.

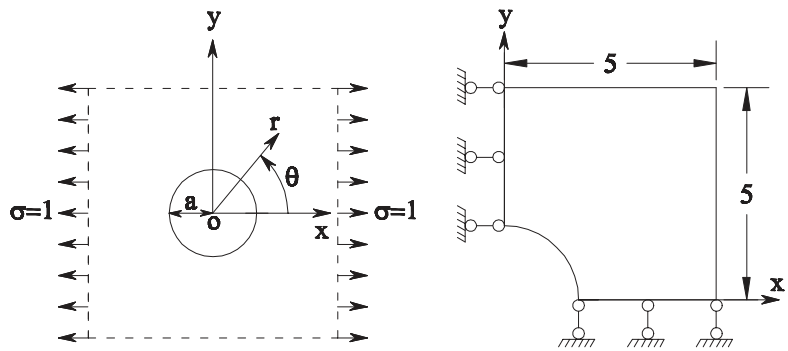


Fig. 12. Infinite plate with a circular hole and its quarter model.

infinity in the $x$-direction, as shown in Fig. 12. Due to its symmetry, only the upper right quadrant of the plate is modeled. Plane strain condition is considered, $E = 1.0 \times 10^3\,\mathrm{N/m^2}$, $\nu = 0.3$, and the central circular hole is of radius $a = 1\,\mathrm{m}$. Symmetric conditions are imposed on the left and bottom edges, and the inner boundary of the hole is traction free. The exact solution for the stress is

[Timoshenko and Goodier (1970)]

$$\begin{aligned}
\sigma_{11} &= 1 - \frac{a^2}{r^2}\left[\frac{3}{2}\cos 2\theta + \cos 4\theta\right] + \frac{3a^4}{2r^4}\cos 4\theta \\
\sigma_{22} &= -\frac{a^2}{r^2}\left[\frac{1}{2}\cos 2\theta - \cos 4\theta\right] - \frac{3a^4}{2r^4}\cos 4\theta \quad , \\
\tau_{12} &= -\frac{a^2}{r^2}\left[\frac{1}{2}\sin 2\theta + \sin 4\theta\right] + \frac{3a^4}{2r^4}\sin 4\theta
\end{aligned} \tag{82}$$

where $(r, \theta)$ are the polar coordinates and $\theta$ is measured counterclockwise from the positive $x$-axis. Traction boundary conditions are imposed on the right ($x = 5.0$) and top ($y = 5.0$) edges based on the exact solution Eq. (82). The displacement components corresponding to the stresses are

$$\begin{aligned}
u_1 &= \frac{a}{8\mu}\left[\frac{r}{a}(\kappa+1)\cos\theta + 2\frac{a}{r}((1+\kappa)\cos\theta + \cos 3\theta) - 2\frac{a^3}{r^3}\cos 3\theta\right] \\
u_2 &= \frac{a}{8\mu}\left[\frac{r}{a}(\kappa-1)\sin\theta + 2\frac{a}{r}((1-\kappa)\sin\theta + \sin 3\theta) - 2\frac{a^3}{r^3}\sin 3\theta\right],
\end{aligned} \tag{83}$$

where $\mu = E/(2(1+\nu))$, $\kappa$ is defined in terms of Poisson's ratio by $\kappa = 3 - 4\nu$ for plane strain cases.

We first use the SFEM with quadrilateral elements to perform the analysis with two smoothing cells in an element. The numerical strain energies have been plotted against the DOFs in Fig. 13 with the FEM solution obtained using the same mesh.

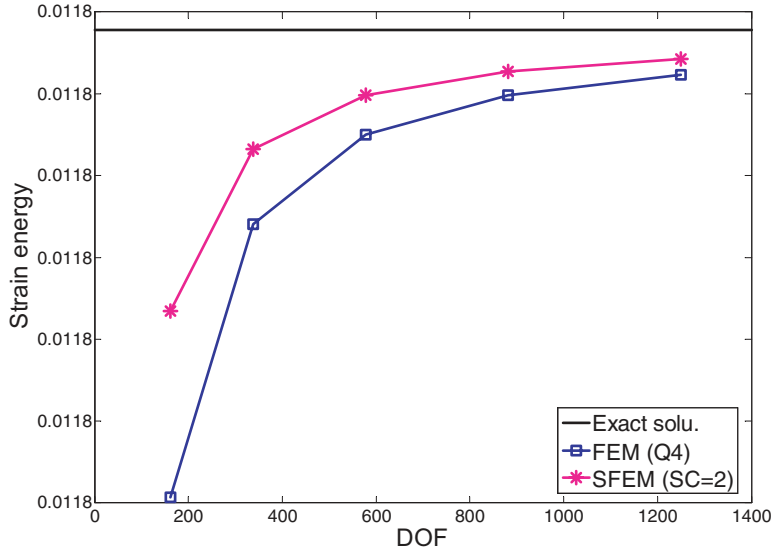


Fig. 13. Solutions for the plate-with-hole obtained using FEM, SFEM with two smoothing cells in an element and the same triangular mesh in comparison with the exact solution.

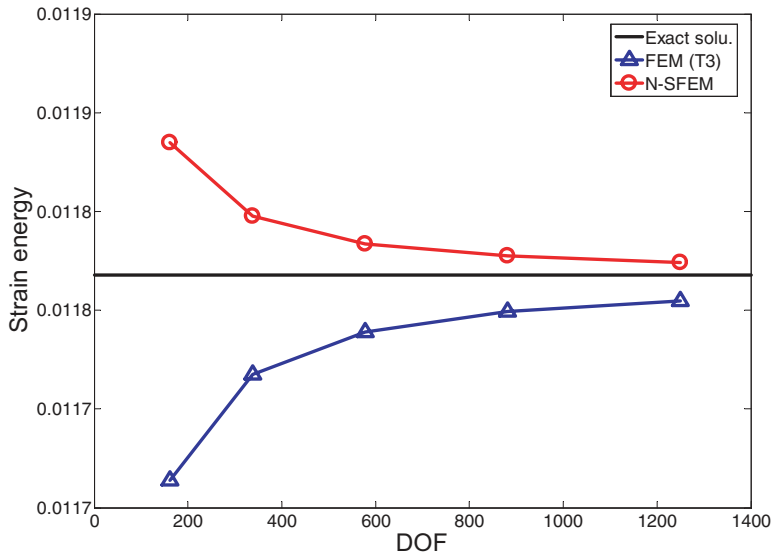


Fig. 14. Solutions for the plate-with-hole obtained using FEM, N-SFEM and the same triangular mesh in comparison with the exact solution.

It is seen that the SFEM does not produces upper bound solution for this problem. It produces a tighter lower bound solution compared to the FEM solution, which confirms Theorem 5.4.

We next use the N-SFEM with triangular elements to perform the analysis with one smoothing cell/domain for each node. The numerical strain energies have been plotted against the DOFs in Fig. 14 with the FEM solution obtained using the same mesh and the same set of nodes. It is found that the N-SFEM can still produce upper bound solution for this problem.

We finally use the NS-PIM with triangular elements to perform the same analysis with one smoothing cell/domain for each node. The numerical strain energies have been plotted against the DOFs in Fig. 15 with the FEM solution obtained using the same mesh and the same set of nodes.

In summary, for the plate-with-hole problem, only the N-SFEM and NS-PIM can produce upper bound solutions. This is because the node-based smoothing provides sufficient softening effects. For all the examples studied using the N-SFEM and NS-PIM upper bound solutions were obtained without exception.

### 6.3. *Application to an offshore structure: a riser connector*

The 3D codes of NS-PIM and E-SFEM have also been developed. Here we present one example of NS-PIM applied to solve a real offshore structure problem of a Floating Production and Storage Unit (FPSO). Fluid transfer of oil-gas-water mixture between FPSO and subsea pipeline is carried out through a riser attached to

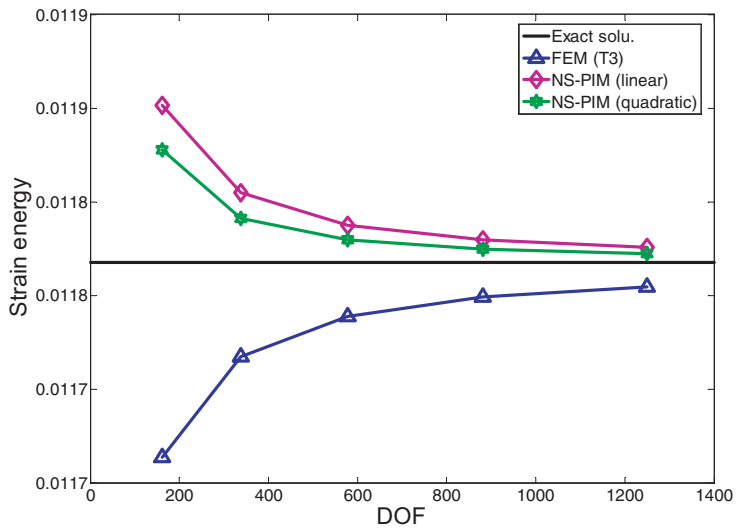


Fig. 15. Solutions for the plate-with-hole obtained using FEM, NS-PIM and the same triangular mesh in comparison with the exact solution. For the case of quadratic NS-PIM, 6 nodes are used in the interpolation in an overlapping manner, and hence same triangular mesh of some number of nodes can be used.

FPSO shipside by the riser connector. The simplified model of riser connector is shown in Fig. 15 with the load being applied on the top flange of riser connector. The boundary conditions are defined at the end of I-beams where riser connector is supported by other structures. This riser connector is made of steel material with Young's modulus $E = 2.0 \times 10^5\,\mathrm{N/mm^2}$, Poisson's ratio $\nu = 0.32$. The results of a contour of elemental Von Mises stress are plotted in Fig. 16 in the deformed shape of the riser connector.

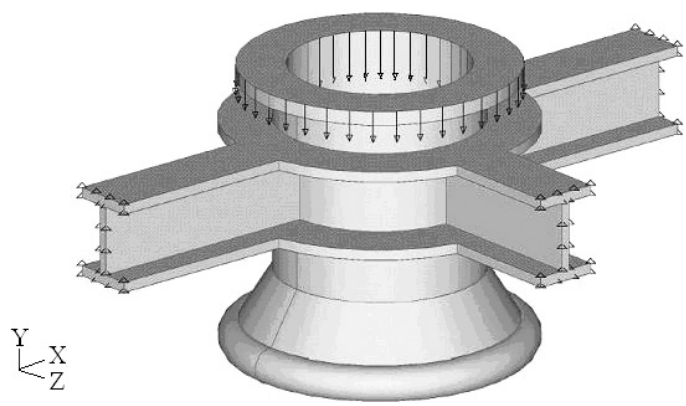


Fig. 16. Simplified model of a three-dimensional riser connector.

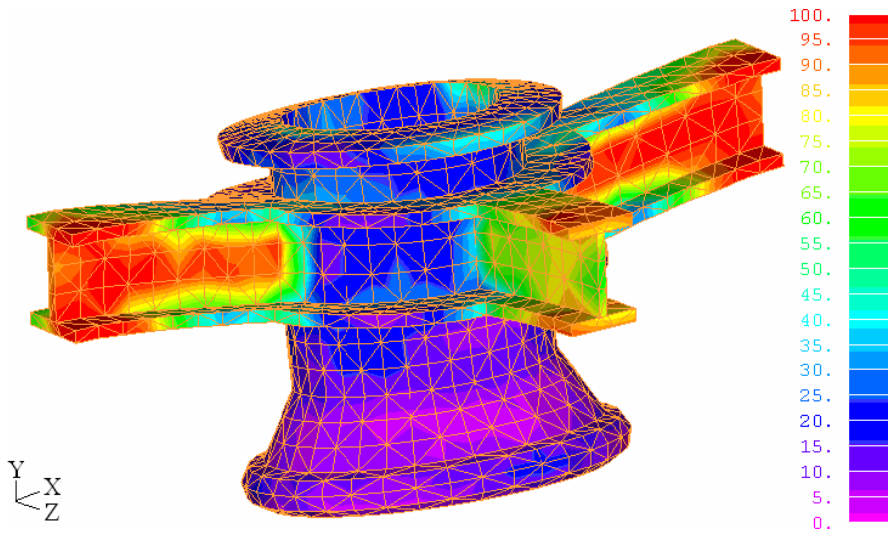


Fig. 17. Contour of the Von Mises stress obtained using a 3D NS-PIM code.

## 7. Conclusion

In this work, we introduce a generalized gradient smoothing technique, corresponding smoothed bilinear form with different smoothing domains, and proved the important general properties. The smoothed bilinear form is then used to formulate a smoothed Galerkin weakform that is applicable for establishing a class of numerical methods. The smoothed Galerkin weakform is proven to be a unique alternative for establishing numerical methods for stable (bounded) and monotonically convergent solutions. The smoothed bilinear form establishes a unified theoretical foundation for a class of methods that can produce upper bound solutions (in energy norm) for solid mechanics problems. The bilinear form has the following properties.

(1) It has the basic properties of positivity and symmetry.
(2) It can have bound properties.
(3) It further relates the requirement of the assumed solution space.
(4) It is capable of establishing numerical methods that produce solutions of both upper and lower bounds, supper-convergence, ultra accuracy and other desired properties by properly choosing smoothing cells/domains.

The numerical methods developed based on this smoothed bilinear form, such as the NS-PIM, N-SFEM and E-SFEM, possess three major important features

(1) The stiffness of the discretized model will be reduced compared to the FEM model and the exact model, which allows us to obtain upper bound solutions with respect to both the FEM solution and the exact solution;

(2) The E-SFEM using triangular mesh can produce solutions of ultra accuracy that is even more accurate that the FEM solution using quadrilateral elements.
(3) The continuity of the trial and test functions can be reduced, which allows us to use much more types of methods to create shape functions;
(4) The solution of a numerical method developed using the smoothed bilinear form is insensitive to the quality of the mesh, and triangular meshes can be used perfectly without any problems.
(5) There is no increase in the number of the unknowns and the primary variable is still the nodal displacements. The discrete system equations are symmetrical and sparse with the same dimension as that of the FEM and hence the same order in computational efficiency.

Based on the general techniques and theory established in this paper, we can expect also that by changing the smoothing function, the ways for the smoothing domain/cell construction, and the use of different shape functions, better numerical methods with desired properties can be developed. A combined formulation of the (fully-compatible) Galerkin weakform and the smoothed Galerkin weakform offers also possibilities for developing numerical methods with supper-convergence property. This is because the Galerkin weakform gives lower bound and the smoothed Galerkin weakform provide upper bound of the exact solution, and therefore there must be way to obtain an ultra accurate solution that is very close to the exact solution, and solutions of very fast convergence (Liu, Nguyen and Lam, 2008c).

Finally, we would like to mention that the properties of the generalized bilinear form for functions in the finite element solution space are becoming clearer recently for linear elements for the works on SFEM, N-SFEM and E-SFEM. More works, however, need to be done for higher order elements. In the $G^1$ space, however, it requires a lot more detailed and in-depth study and analysis. So far we have results only for NS-PIM with quadratic interpolation and radial PIM interpolations. We found the results are good for these cases, as presented in this paper and in [Liu and Zhang (2005, 2008); Liu and Li (2006); Zhang *et al.* (2007); Li *et al.* (2007)], but we do not know precisely how good and why they are good. There are a lot of issues needs to investigate in these related areas including new territories of functional analysis for discommodious functions, and the author is still trying hard to study, examine and understand them. Hopefully, some new interesting properties may be found when more study is conducted by the author's group and possibly by other groups in world.

**Acknowledgements**

The author would like to thank Dr. Zhang GY and Mr. T. Nguyen-Thoi for their comments and suggestions and running of these example problems for this paper. Thanks are extended also to many other members at ACES who have offered comments and suggestions to this work.

## References

Chen, J. S., Wu, C. T. and Belytschko, T. [2000] Regularization of material instabilities by meshfree approximations with intrinsic length scales, *International Journal for Numerical Methods in Engineering* **47**, 1303–1322.

Chen, J. S., Wu, C. T., Yoon, S. and You, Y. [2001] A stabilized conforming nodal integration for Galerkin mesh-free methods, *International Journal for Numerical Methods in Engineering* **50**, 435–466.

Dai, K. Y., Liu, G. R. and Nguyen, T. T. [2007] An n-sided polygonal smoothed finite element method (nSFEM) for solid mechanics, *Finite Elements in Analysis and Design* **43**, 847–860.

Dohrmann, C. R., Heinstein, M. W., Jung, J., Key, S. W. and Witkowski, W. R. [2000] Node-based uniform strain elements for three-node triangular and four-node tetrahedral meshes, *International Journal for Numerical Methods in Engineering* **47**, 1549–1568.

Eringen, A. C. and Edelen, D. G. B. [1972] On nonlocal elasticity, *Int. J. Eng. Sci.* **10**, 233–248.

Hughes, T. J. R. [1987] *The Finite Element Method* (Prentice-Hall, London).

Li, Y., Liu, G. R., Luan, M. T., Dai, K. Y., Zhong, Z. H., Li, G. Y. and Han, X. [2007] Contact analysis for solids based on linearly conforming radial point interpolation method, *Computational Mechanics* **39**, 537–554.

Liu, G. R. and Gu, Y. T. [2001] A point interpolation method for two-dimensional solids, *International Journal for Numerical Methods in Engineering* **50**, 937–951.

Liu, G. R. [2002] *Meshfree Methods: Moving Beyond the Finite Element Method* (CRC Press: Boca Raton, USA).

Liu, G. R. and Liu, M. B. [2003] *Smoothed Particle Hydrodynamics — A Meshfree Particle Method* (World Scientific: Singapore).

Liu, G. R. and Quek, S. S. [2003] *Finite Element Method: A Practical Course* (Butter-Worth-Heinemann, Burlington, MA).

Liu, G. R. and Gu, Y. T. [2005] *An Introduction to MFree Methods and Their Programming* (Springer).

Liu, G. R., Zhang, G. Y., Dai, K. Y., Wang, Y. Y., Zhong, Z. H., Li, G. Y. and Han, X. [2005] A linearly conforming point interpolation method (LC-PIM) for 2D mechanics problems, *International Journal for Computational Methods* **2**, 645–665.

Liu, G. R., Li, Y., Dai, K. Y., Luan, M. T. and Xue, W. [2006] A linearly conforming radial point interpolation method for solid mechanics problems, *International Journal of Computational Methods* **3**, 401–428.

Liu, G. R., Dai, K. Y. and Nguyen, T. T. [2007] A smoothed finite element method for mechanics problems, *Computational Mechanics* **39**, 859–877.

Liu, G. R., Nguyen, T. T., Dai, K. Y. and Lam, K. Y. [2007a] Theoretical aspects of the smoothed finite element method (SFEM), *International Journal for Numerical Methods in Engineering* **71**, 902–930.

Liu, G. R., Nguyen, T. T., Nguyen, X. H. and Lam, K. Y. [2007b] A node-based smoothed finite element method (N-SFEM) for upper bound solutions to solid mechanics problems, *Computers and Structures* (submitted).

Liu, G. R. and Zhang, G. Y. [2008] Upper bound solution to elasticity problems: A unique property of the linearly conforming point interpolation method (LC-PIM), *Int. J. Numer. Mech. Engrg.* **74**, 1128–1161.

Liu, G. R., Nguyen, T. T. and Lam, K. Y. [2008a] An edge-based smoothed finite element method (E-SFEM) for static and dynamic problems of solid mechanics, *J. Sound. Vib.* (submitted).

Liu, G. R., Nguyen, T. T. and Lam, K. Y. [2008b] An assumed strain FEM by scaling the gradient of strains with scaling factor $\alpha$ ($\alpha$FEM) *Computational Mechanics* (accepted).

Liu, G. R., Nguyen, T. T. and Lam, K. Y. [2008c] A novel Alpha Finite Element Method ($a$FEM) for exact solution to mechanics problems using triangular and tetrahedral elements, *Computer Methods in Applied Mechanics and Engineering* (accepted).

Liu, G. R., Xu, X., Zhang, G. Y. and Nguyen, T. T. [2008] A superconvergent point interpolation method (SC-PIM) with piecewise linear strain field using triangular mesh, *International Journal for Numerical Methods in Engineering* (revised).

Lucy, L. B. [1977] Numerical approach to testing the fission hypothesis, *Astronomical Journal* **82**, 1013–1024.

Monaghan, J. J. [1982] Why particle methods work (hydrodynamics), *SIAM Journal on Scientific and Statistical Computing* **3**, 422–433.

Oliveira Eduardo, R. and De Arantes, E. [1968] Theoretical foundations of the finite element method, *International Journal of Solids and Structures* **4**, 929–952.

Ortega, E., Oñate, E. and Idelsohn, S. [2007] An improved finite point method for tridimensional potential flows, *Comput. Mech.* **40**, 949–963, available on line: DOI: 10.1007/s00466-006-0154-6.

Pian, T. H. H. and Wu, C. C. [2006] *Hybrid and Incompatible Finite Element Methods* (CRC Press, Boca Raton).

Simo, J. C. and Hughes, T. J. R. [1998] *Computational Inelasticity* (Springer-Verlag: New York).

Timoshenko, S. P. and Goodier, J. N. [1970] *Theory of Elasticity* (3rd ed) (McGraw-Hill: New York).

Wang, J. G. and Liu, G. R. [2002] A point interpolation meshless method based on the radial basis functions, *International Journal for Numerical Methods in Engineering* **54**, 1623–1648.

Wu, H. C. [1982] *Variational Principle in Elasticity and Applications* (Scientific Press: Beijing).

Zhang, Y. Q., Liu, G. R. and Han, X. [2006] Effect of small length scale on elastic buckling of multi-walled carbon nanotubes under radial pressure, *Physics Letters A* **349**, 370–376.

Zhang, G. Y., Liu, G. R., Nguyen, T. T., Song, C. X., Han, X., Zhong, Z. H. and Li, G. Y. [2007] The upper bound property for solid mechanics of the linearly conforming radial point interpolation method (LC-RPIM), *International Journal of Computational Methods* **4**(3), 521–541.

Zhang, G. Y., Liu, G. R., Wang, Y. Y., Huang, H. T., Zhong, Z. H., Li, G. Y. and Han, X. [2007] A linearly conforming point interpolation method (LC-PIM) for three-dimensional elasticity problems, *International Journal for Numerical Methods in Engineering* **72**, 1524–1543.